

**TOWARD UNDERSTANDING THE BREAKING
MECHANISM OF VISCOELASTIC SURFACTANT IN
WELL STIMULATION**

BY

LIONEL TALLEY FOGANG

A Thesis Presented to the
DEANSHIP OF GRADUATE STUDIES

KING FAHD UNIVERSITY OF PETROLEUM & MINERALS

DHAHRAN, SAUDI ARABIA

In Partial Fulfillment of the
Requirements for the Degree of

MASTER OF SCIENCE

In

PETROLEUM ENGINEERING

DECEMBER 2015

KING FAHD UNIVERSITY OF PETROLEUM & MINERALS

DHAHRAN- 31261, SAUDI ARABIA

DEANSHIP OF GRADUATE STUDIES

This thesis, written by **LIONEL TALLEY FOGANG** under the direction his thesis advisor and approved by his thesis committee, has been presented and accepted by the Dean of Graduate Studies, in partial fulfillment of the requirements for the degree of **MASTER OF SCIENCE IN PETROLEUM ENGINEERING.**

443

Dr. ABDULLAH S. SULTAN
Department Chairman

Dr. Salam A. Zummo
Dean of Graduate Studies

22/5/16

Date

443

Dr. ABDULLAH S. SULTAN
(Advisor)

Dr. SIDQI ABU-KHAMSIN
(Member)

Mohamed Mahmoud

Dr. MOHAMED MAHMOUD
(Member)

Hussein

Dr. IBNELWALEED ALI
HUSSEIN
(Member)

Shakil

Dr. SYED SHAKIL HUSSAIN
(Member)

© Lionel Talley Fogang

2015

This thesis is dedicated to my parents, siblings and extended family

ACKNOWLEDGMENTS

I thank King Fahd University of Petroleum & Minerals (KFUPM) for giving me the opportunity to study Petroleum Engineering as both a Bachelor and Master student. I thank the Center for Integrative Petroleum Research (CIPR, formerly known as the Center for Petroleum and Minerals) for providing me the post of Research Assistant during my time as a Masters Student.

I am very grateful to Dr. Abdullah Sultan, the Chairman of the Petroleum Department, and the Director of the CIPR, for all the guidance and support he has given me since my undergraduate years, despite his duties.

I express my gratitude to Dr. Sidqi Abu-Khamsin who advised me during my undergraduate years. His advice and support enabled me to graduate and continue a Master program at KFUPM.

I thank Dr. Syed Shakil of the CIPR for giving me the necessary knowledge I needed for my thesis work. I thank Dr. Kamal Shahzad for also providing me insights on how to structure my report.

I thank Mr. Abdul Samed who helped me adapt to the new environment during my first years as an undergraduate student. I also thank him and Mr. Mohammadin for their help and advice while I worked in the laboratory. I thank Dr. Musa Musa of the Chemistry Department, Dr. Mamdouh Al-Harthi and Dr. Ibneelwaleed Ali Hussein of the Chemical Engineering Department for their permission to work in their laboratories so that I could finish my work. I acknowledge Akzo Nobel for providing me the samples to do the

experiment. I thank the Laboratory for Advanced Microscopy of the Nanoscience Institute of Aragon (LMA-INA), Spain, for the Transmission Electron Microscopy studies. I thank my thesis committee members, Dr. Abdullah Sultan, Dr. Sidqi Abu-Khamsin, Dr. Mohamed Mahmoud, Dr. Ibnelwaleed Hussein, and Dr. Syed Shakil, for their time to listen and judge my work.

I thank my father for his contributions in making this report readable. I thank my mother who called to know my progress and gave me moral support during my work. I thank my siblings and extended family for contacting me during this period. I thank Mr. Najmudeen Sibaweihi, Mr. Soh Edwin, Mr. Umaru, Mr. Kamal Mende, and others who I cannot list for lack of space, for their encouragement. Special thanks go to my friend and classmate, Mr. Noor Ahmed Shinwari, and Dr. Mohammed Hamdan of the Physical Education Department, who were instrumental to my rapid completion. Mr. Omar Duhaibi also gets my appreciation for the Arabic translation of the abstract.

Finally, but most importantly, I am grateful to the Creator of the Universe for providing those who supported me and I the resources I needed to complete this work. These resources include generosity, patience, finance, health, strength, empathy, and our reasoning faculties.

TABLE OF CONTENTS

| | |
|---|------|
| ACKNOWLEDGMENTS | V |
| TABLE OF CONTENTS..... | VII |
| LIST OF TABLES..... | IX |
| LIST OF FIGURES..... | X |
| LIST OF ABBREVIATIONS..... | XIII |
| ABSTRACT | XIV |
| ملخص الرسالة | XVI |
| CHAPTER 1 INTRODUCTION..... | 1 |
| 1.1 Statement of the Problem..... | 3 |
| 1.2 Objectives | 4 |
| 1.3 Thesis Organization..... | 4 |
| CHAPTER 2 LITERATURE REVIEW | 5 |
| 2.1 VES Applications in the Petroleum Industry | 5 |
| 2.1.1 Micelle Formation | 5 |
| 2.2 Breaker Application in the Petroleum Industry | 8 |
| 2.3 Experimental Details and Proposed Breaking Mechanisms | 9 |
| CHAPTER 3 THEORITCAL BACKGROUND | 15 |
| 3.1 Rheology..... | 15 |
| 3.1.1 Theory of Maxwellian Fluids..... | 16 |
| 3.1.2 Theory of viscoelastic surfactants rheology | 17 |

| | |
|--|-----------|
| 3.2 Cryogenic Transmission Electron Microscopy (Cryo-TEM) | 18 |
| CHAPTER 4 EXPERIMENTAL PROCEDURE..... | 20 |
| 4.1 Materials..... | 20 |
| 4.2 Sample Preparation | 21 |
| 4.3 Rheology..... | 21 |
| 4.4 Cryo-TEM | 22 |
| CHAPTER 5 RESULTS AND DISCUSSIONS | 27 |
| 5.1 Rheology of surfactant solution without organic compounds | 27 |
| 5.2 Rheology of surfactant solution with the organic compounds | 36 |
| 5.2.1 Effect of the oils | 36 |
| 5.2.2 Effect of PGA | 57 |
| 5.3 Implications for well stimulation..... | 59 |
| CHAPTER 6 CONCLUSIONS | 63 |
| REFERENCES..... | 65 |
| VITAE | 70 |

LIST OF TABLES

| | |
|---|----|
| Table 1 Extra virgin olive oil composition | 26 |
| Table 2 Crude Oil composition..... | 26 |
| Table 3 Estimated values of crossover frequency and relaxation time of the pure surfactant solution | 32 |
| Table 4 Estimated differences in zero-shear viscosities between the VES solutions with the oils and the pure VES solutions at test temperatures | 38 |

LIST OF FIGURES

| | |
|---|----|
| Figure 1 Schematic diagram of individual surfactant monomers and surfactant micelle [20]..... | 7 |
| Figure 2 Packing parameter and corresponding micelle structure [24, p. 2] | 7 |
| Figure 3 Chemical structure of erucamidopropyl hydroxypropyl sulfobetaine [52] | 23 |
| Figure 4 Chemical structure of n-decane | 23 |
| Figure 5 Chemical structure of polyglycolic acid..... | 23 |
| Figure 6 Chemical structure of glycerol | 23 |
| Figure 7 Chemical structure of palmitic acid..... | 24 |
| Figure 8 Chemical structure of stearic acid | 24 |
| Figure 9 Chemical structure of oleic acid..... | 24 |
| Figure 10 Chemical structure of palmitoleic acid..... | 24 |
| Figure 11 Chemical structure of linoleic acid..... | 25 |
| Figure 12 Chemical structure of α -linolenic acid | 25 |
| Figure 13 Chemical structure of triolein..... | 25 |
| Figure 14 Zero-shear viscosity of surfactant solution with time | 30 |
| Figure 15 Viscosity vs shear rate of 3.96 wt % surfactant solution..... | 30 |
| Figure 16 Viscosity vs shear stress of 3.96 wt % surfactant solution..... | 31 |
| Figure 17 Shear stress vs shear rate of 3.96 wt % surfactant solution..... | 31 |
| Figure 18 Storage modulus (filled symbols) and loss modulus (open symbols) of 3.96 wt % surfactant solution..... | 32 |
| Figure 19 Cryo-TEM image of 3.96 wt % surfactant solution at 30°C. The black curves represent the edges of the micelles..... | 33 |
| Figure 20 Cryo-TEM image of 3.96 wt % surfactant solution at 30°C diluted in ethyl acetate. The black curves represent the edges of the micelles..... | 34 |
| Figure 21 Cryo-TEM image of 3.96 wt % surfactant solution at 30°C diluted in ethyl acetate. The black curves represent the edges of the micelles..... | 35 |
| Figure 22 Estimated zero-shear viscosity of 3.96 wt % surfactant solution with different n-decane concentrations with the lines as visual aids. The full lines link the points at 30°C, whereas the dashed lines link the points at 60°C | 37 |
| Figure 23 Estimated zero-shear viscosity of 3.96 wt % surfactant solution with different crude oil concentrations with the lines as visual aids. The full lines link the points at 30°C, whereas the dashed lines link the points at 60°C | 37 |
| Figure 24 Estimated zero-shear viscosity of 3.96 wt % surfactant solution with different EVOO concentrations with the lines as visual aids. The | |

| | |
|--|----|
| full lines link the points at 30°C, whereas the dashed lines link the points at 60°C | 38 |
| Figure 25 Schematic showing the migration of oil molecules (small strands) from an oil droplet (gray region) to a cylindrical micelle after adsorption of the micelle on the oil-aqueous solution interface..... | 39 |
| Figure 26 Viscosity vs shear rate of 3.96 wt % surfactant solution with different concentrations of n-decane at 30°C | 43 |
| Figure 27 Viscosity vs shear rate of 3.96 wt % surfactant solution with different concentrations of crude oil at 30°C | 43 |
| Figure 28 Viscosity vs shear rate of 3.96 wt % surfactant solution with different concentrations of EVOO at 30°C | 44 |
| Figure 29 Viscosity vs shear rate of 3.96 wt % surfactant solution with different concentrations of n-decane at 60°C | 44 |
| Figure 30 Viscosity vs shear rate of 3.96 wt % surfactant solution with different concentrations of crude oil at 60°C | 45 |
| Figure 31 Viscosity vs shear rate of 3.96 wt % surfactant solution with different concentrations of EVOO at 60°C | 45 |
| Figure 32 Storage modulus (filled symbols) and loss modulus (open symbols) of 3.96 wt % surfactant solution with different concentrations of n-decane at 30°C..... | 46 |
| Figure 33 Storage modulus (filled symbols) and loss modulus (open symbols) of 3.96 wt % surfactant solution with different concentrations of crude oil at 30°C..... | 46 |
| Figure 34 Storage modulus (filled symbols) and loss modulus (open symbols) of 3.96 wt % surfactant solution with different concentrations of EVOO at 30°C..... | 47 |
| Figure 35 Storage modulus (filled symbols) and loss modulus (open symbols) of 3.96 wt % surfactant solution with different concentrations of n-decane at 60°C..... | 47 |
| Figure 36 Storage modulus (filled symbols) and loss modulus (open symbols) of 3.96 wt % surfactant solution with different concentrations of crude oil at 60°C..... | 48 |
| Figure 37 Storage modulus (filled symbols) and loss modulus (open symbols) of 3.96 wt % surfactant solution with different concentrations of EVOO at 60°C..... | 48 |
| Figure 38 Shear stress vs shear rate of 3.96 wt % surfactant solution with different concentrations of n-decane at 30°C | 49 |
| Figure 39 Shear stress vs shear rate of 3.96 wt % surfactant solution with different concentrations of crude oil at 30°C | 49 |

| | |
|--|----|
| Figure 40 Shear stress vs shear rate of 3.96 wt % surfactant solution with different concentrations of EVOO at 30°C | 50 |
| Figure 41 Shear stress vs shear rate of 3.96 wt % surfactant solution with different concentrations of n-decane at 60°C | 50 |
| Figure 42 Shear stress vs shear rate of 3.96 wt % surfactant solution with different concentrations of crude oil at 60°C | 51 |
| Figure 43 Shear stress vs shear rate of 3.96 wt % surfactant solution with different concentrations of EVOO at 60°C | 51 |
| Figure 44 Viscosity and stress vs shear rate of 3.96 wt % surfactant solution with 0.25 wt% crude oil at 30°C. | 52 |
| Figure 45 Viscosity and stress vs shear rate of 3.96 wt % surfactant solution with 0.25 wt% EVOO at 30°C | 52 |
| Figure 46 Cryo-TEM image of 3.96 wt % surfactant solution with 0.9 wt % n-decane at 30°C. The black curves are the edges of the micelles..... | 54 |
| Figure 47 Cryo-TEM image of 3.96 wt % surfactant solution with 3 wt % n-decane at 60°C. The white sections represent the micelles..... | 55 |
| Figure 48 Schematic of the effect of (i) 3 wt % n-decane and (ii) 3 wt % crude oil and EVOO on the cylindrical micelles at 60°C | 56 |
| Figure 49 Schematic representation of micelle transitions induced by the oils at 30°C and 60°C..... | 56 |
| Figure 50 Viscosity vs shear rate of 3.96 wt % surfactant solution with different concentrations of PGA at 30°C | 60 |
| Figure 51 Viscosity vs shear rate of 3.96 wt % surfactant solution with different concentrations of PGA at 60°C | 60 |
| Figure 52 Estimated zero-shear viscosity of 3.96 wt % surfactant solution with different PGA concentrations..... | 61 |
| Figure 53 Storage modulus (filled symbols) and loss modulus (open symbols) of 3.96 wt % surfactant with different concentrations of PGA at 30°C..... | 61 |
| Figure 54 Storage modulus (filled symbols) and loss modulus (open symbols) of 3.96 wt % surfactant with different concentrations of PGA at 60°C..... | 62 |
| Figure 55 Schematic representing the effect of 0.9 wt % PGA on the cylindrical micelles at 60°C | 62 |

LIST OF ABBREVIATIONS

| | | |
|-----------------|---|---|
| CMC | : | Critical Micelle Concentration |
| VES | : | Viscoelastic Surfactants |
| Cryo-TEM | : | Cryogenic Transmission Electron Microscopy |
| SDA | : | Self-Diverting Acid |
| PEG | : | Polyethylene Glycol |
| PPG | : | Polypropylene Glycol |
| NMR | : | Nuclear Magnetic Resonance |
| SANS | : | Small Angle Neutron Scattering |
| EDAB | : | Erucyl Dimethyl Amidopropyl Betaine |
| SAXS | : | Small Angle X-Ray Scattering |
| PGA | : | Polyglycolic Acid |
| EDAS | : | 3-(N-erucamidopropyl-N,N-dimethyl ammonium) propane sulfonate |
| EMAO | : | Erucyldimethyl amidopropyl amine oxide |
| CCD | : | Charge-Coupled Device Cameras. |
| HVR | : | High viscosity regime |
| TR | : | Transition Regime |
| LVR | : | Low viscosity regime |

ABSTRACT

Full Name : Lionel Talley Fogang

Thesis Title : Toward understanding the breaker mechanism of viscoelastic surfactant in well stimulation

Major Field : Petroleum Engineering

Date of Degree : [December 2015]

Viscoelastic surfactants (VES) gels are used as acid diverters in well stimulation, whereas internal breakers are compounds which reduce the viscosity of these gels after acid diversion. Internal breakers reduce formation damage induced by VES gels. Proposed mechanisms of viscosity reduction of VES gels by internal breakers at high temperatures are not well understood. This study attempted to understand the viscosity reduction mechanism of a certain long-tail sulfobetaine surfactant solution, erucamidopropyl hydroxypropyl sulfobetaine, using organic compounds. This surfactant was within a system containing other compounds. Rheology and cryogenic transmission electron microscopy (cryo-TEM) were used to study the effect of the following organic compounds on a fixed concentration of an aqueous surfactant solution (3.96 wt % of the surfactant system) at 30°C and 60°C: n-decane, crude oil, extra virgin olive oil, and polyglycolic acid (PGA). All the samples were equilibrated for a week. The solution was viscoelastic and highly viscous at both temperatures due to the presence of cylindrical micelle networks. Only n-decane drastically affected the zero-shear viscosity of the surfactant solution at 30°C. The zero-shear viscosity of the surfactant solution

reduced with increasing concentration of the oils by approximately three to five orders of magnitude at 60°C. N-decane induced three regimes of viscosity change at both temperatures: the high viscosity regime, the transition regime, and the low viscosity regime. The other oils induced only one and two regimes of viscosity change at 30°C and 60°C, respectively. PGA did not induce considerable changes in viscosity at both temperatures. In conclusion, the oils are breakers for this VES solution. Moreover, temperature and oil molecular structure do govern the viscosity reduction of the solution. Meanwhile, PGA is not a compound to be used with this VES solution.

ملخص الرسالة

الاسم الكامل: ليونيل تالي فوغانغ

عنوان الرسالة: نحو فهم آلية تكسير المسيبات اللزجة المطاطية حال تنشيطها آبار النفط

التخصص: هندسة بترول

تاريخ الدرجة العلمية: ديسمبر 2015

مما يُستعمل لتنشيط آبار النفط خافضات توتر الأسطح (المسيبات) اللزجة المطاطية (VES) ممزوج معها فواصل أو كسارات (Internal Breakers)؛ بحيث تحوّل المسيبات مسار الأحماض داخل الممكن بينما تقلّل الكسارات لزوجة المسيبات لتقلّل ضرر التصاقها بأسطح الصخر المحيط بالبئر. إن الآليات المقترحة لتقليل لزوجة المسيبات في حرارة عالية غير مفهومة حقاً. لذا نحاول في بحثنا هذا فهم آليات تقليل لزوجة أحد مركبات المسيبات من مجموعة الكبريتوبيتاين طويلة السلسلة -تحديداً هو إبروسيل أميد البروبيل هيدروكسي بروبيل كبريتوبيتاين- عن طريق مركبات عضوية. اخترنا لهذا البحث أربع مركبات عضوية -ثلاثة زيوت وحمضاً- هي: الديكان، و النفط الخام، و زيت الزيتون البكر الممتاز، و حمض عديد الغليكوليك، لندرس أثرها على محلول مائي للمسيب المذكور يبلغ تركيزه (3.96 % وزناً) عند كل من درجتَي 30°م و 60°م باستخدام علم انسياب الموائع و تقنية مجهرية هي نقل الإلكترونات في وسط شديد البرودة تسمى (cryo-EM)، و تُركت عيّات محلول المسيب ساكنة أسبوعاً قبل بدء التجربة. في تجاربنا بقي المحلول مطاطاً و عاليّ اللزوجة في كلا درجتَي الحرارة بسبب احتوائه هياكل ميسيلية اسطوانية. ثم لم يؤثر في لزوجة المسيب حال سكونه عند 30°م إلا الديكان، أما عند 60°م فقد قلّت الزيوت الثلاثة كلّها هذه اللزوجة أطراداً مع تركيزها بما يقرب من آلاف المرات إلى عشرات الآلاف. ثم بمراقبة أنماط أثر المواد الأربعة في تقليل اللزوجة وجدنا أثر الديكان عند كلا درجتَي الحرارة واقعا في ثلاث مناطق: منطقة لزوجة عالية، و منطقة انتقال وسيطة، و منطقة لزوجة منخفضة. و أما الزيتان الآخران فأثرهما عند 30°م وقع في منطقة واحدة، و عند

60°م في منطقتين. و أما الحمض فلم يؤثر تأثيرا في اللزوجة تحت كلا درجتي الحرارة. نخلص إلى أن هذه الزيوت كسارات لهذا المسيب اللزج، و أن كلاً من الحرارة و هيكله جزيئات الزيت يحكم تقليل لزوجة المسيب، و أن حمض عديد الغليكوليك لا ينفع استخدامه مع هذا المسيب تحديداً.

CHAPTER 1

INTRODUCTION

The word “surfactant” is a short form for surface active agents [1, p. 1]. They are amphiphilic compounds because they have both water-loving (hydrophilic) and water-hating (hydrophobic) regions. The hydrophilic region is a headgroup while the hydrophobic region is a long chain hydrocarbon attached to the headgroup [2]. Their amphiphilic nature makes it possible for them to reduce the interfacial tension between water and air, hence, the reason why they are called surface acting agents [3]. The reduction of interfacial tension is due to adsorption of the surfactants on surfaces [1, p. 1]. Soaps and detergents are common examples of surfactants [2].

The criteria for surfactant classification are the headgroup charge and the number of headgroups. Based on their headgroup charge, surfactants can be cationic, anionic, non-ionic or zwitterionic. Based on the number of heads, they can be classified as single head or gemini surfactants [2], [4].

Viscoelastic surfactants (VES) are surfactants with both viscous and elastic properties. These differ from other surfactants that behave as Newtonian fluids with viscosities marginally higher than that of water [5]. They are used in the petroleum industry for drilling [6], reservoir stimulation [7], and enhanced oil recovery [2]. VES were used together with gravel packs in the 1980s and 1990's for hydraulic fracturing [8], replacing

polymer-based fracturing fluids that were used in the 1970s [7]. A reason for this replacement is that VES gels are easily cleaned up from the formation when compared to polymer fluids [9]. This is because their viscosities are easily reduced when they come in contact with reservoir oil [7].

VES commonly used in oil fields generally have a working temperature range of 160-200°F [10], though some have been used in reservoirs in a range of 250-280°F [11]. Higher salt concentrations improve the stability of VES gels at higher temperatures [9]. VES have also been used in low permeability reservoirs [12], and can be used in tight gas reservoirs as unconventional fracturing fluids [10]. The high viscosity of VES gels gives them the ability to be good fluid leak off controllers, especially in gas reservoirs [11].

In hydraulic fracturing, the fracturing fluid opens up the fracture and transports the proppant materials to keep the fracture open [9]. VES solutions are suitable for hydraulic fracturing because they are highly viscous [9]. The high viscosity enables the creation of a fracture and the carrying of proppant into the created fracture [12]. Moreover, preparation of VES fracturing fluid requires fewer resources than preparing polymer-based fracturing fluids [9]. Minimal pressure drop is needed when pumping VES during the placement of pipes [12]. In matrix acidizing, a VES solution together with an acid is used as an acid diverter [13]. They have been used in oil [14] and gas reservoirs [15].

The term breaker, as used in the petroleum engineering industry, is any compound that reduces the viscosity of any VES solution. Breaking, as used in the petroleum engineering industry, is the process of reducing the viscosity of any VES solution. Breakers are classified into internal and external breakers. The criterion of classification

is how the breaker contacts the VES solution. Internal breakers are mixed together with the VES solution while external breakers contact the viscosified VES solution [8].

Breakers are used in well stimulation along with VES. The use of breakers is necessary as the viscous VES solution can cause formation damage when left in the reservoir [16]. They clean up the formation by reducing the viscosity of the VES gel in order to resume oil production after well stimulation. The external breaker is the reservoir crude oil [7]. Internal breakers have been used in gas reservoirs in the Gulf of Mexico because more efficient gas production was achieved when compared to not using any internal breaker [15]. They are also to be used in tight gas reservoirs [17].

1.1 Statement of the Problem

Several studies have determined the effect of organic compounds that break VES solutions. Most of the discussion on breaking VES solutions has focused on the solubilization site of oils. Recently, more detailed work demonstrated that oil solubilization in the VES solutions depends on energy strains existing in cylindrical micelles [18]. Despite this new insight, most of these studies were conducted at ambient temperatures. Such studies are incomplete for oil field operations that deal with high temperatures. Moreover, most of these studies have not used long-tail surfactant systems developed for oil field applications. Studies conducted at high temperatures using long-tail surfactants do not have detailed breaking mechanisms. Understanding the breaking mechanism of a long-tail VES at high temperatures will help improve well stimulation jobs that require both VES and internal breakers.

1.2 Objectives

The objective of this study was to understand the breaking mechanism of a new class of surfactant by internal breakers after the formation of the viscoelastic gel. This surfactant was a long-tail sulfobetaine developed for reservoir temperatures. The study was conducted at 30°C and 60°C using rheology and cryogenic transmission electron microscopy (cryo-TEM). The effects of four organic compounds on the VES system were compared.

1.3 Thesis Organization

Chapter 2 gives a detailed literature review of VES and breaker applications in the petroleum engineering field. It describes the process of micellization, presents experimental details and the proposed mechanisms of viscosity reduction of VES solutions by several organic compounds. Chapter 3 describes rheology and cryo-TEM and gives the theoretical background used in the study of VES. Chapter 4 describes the experimental procedure used in the study. Chapter 5 presents and discusses the results, and gives implications for well stimulation. Chapter 6 provides the conclusion of the work and recommendations.

CHAPTER 2

LITERATURE REVIEW

2.1 VES Applications in the Petroleum Industry

2.1.1 Micelle Formation

Surfactants contain monomers that aggregate to form spherical micelles at critical micelle concentration (CMC) [19]. This process is called micellization (Figure 1). The forces of interaction that need to be balanced for micellization are hydrophobic, steric, electrostatic, hydrogen bonding and Van der Waal interactions [20]. Micellization is favored mainly by hydrophobic interactions between surfactant tails [20], [21], and disfavored mainly by electrostatic interactions between the polar surfactant heads [20], [21] and steric interactions [20].

Micellization can lead to the formation of different micelle shapes (Figure 2). Micelle shape can be controlled by temperature, salinity, surfactant concentration [19], [20], chemical structure change of micelles, ionic strength, and pH [20]. These conditions affect the value of the packing parameter [19], [21], and defines the shape of a micelle [21]. Packing parameter, p , is given by:

$$p = \frac{v}{al} \quad (1)$$

where v is the volume of the molecule, a is the area of head group (which is not only a geometric parameter), and l is the length of the hydrocarbon tail. Micellar growth is

controlled mainly by the surfactant heads as the heads need to be brought together to reduce the available area per surfactant molecules at the surface [20].

Chang et al. [13], [22] reported a VES system to be used as a self-diverting agent in carbonate reservoirs to improve matrix acidizing jobs. One reason for using this system was to limit the stimulation of water zones, thereby limiting water cut [22]. Chang et al. [23] explained the mechanism of gel formation in a reservoir. The system they used consisted of an amphoteric surfactant, a co-surfactant, an acid, and water. The necessary conditions required for micelle build up in a reservoir are pH and the presence of ions. During matrix acidization, the acid reacts with the formation carbonate rocks, leading to an increase in pH and an increase in the availability of calcium ions. The increase in pH leads to the release of hydrogen ions previously attached to the surfactant and co-surfactant at low pH; a process called deprotonation. The electrostatic repulsion between surfactant heads increases and is reduced by calcium ions released from the acid reaction with formation rock, and the deprotonated co-surfactant. This promotes the micellar transition from spherical to cylindrical micelles [23].

A system containing both acid and VES becomes a self-diverting acid (SDA) when pumped into a reservoir. Unlike external gelling agents that rely on Darcy's Law for propagation as they are gelled before injection, SDAs form a gel in the reservoir, beginning in the high permeability sections. The high viscous gel offers resistance to flow to the SDA of low viscosity behind it. Thus, the ungelled low viscosity SDA follows the path of least resistance by entering the low permeability sections of the reservoirs. This prevents further reaction of the acid with the already formed wormholes [13].

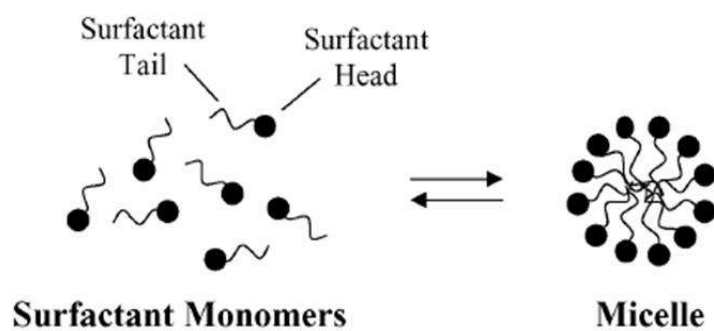


Figure 1 Schematic diagram of individual surfactant monomers and surfactant micelle [20]

| | | | | |
|--------------|--|---|--|--|
| | <p style="text-align: center;">10^0-10^1 nm</p> | <p style="text-align: center;">10^1-10^4 nm</p> <p style="text-align: center;">10^0-10^1 nm</p> | <p style="text-align: center;">10^1-10^5 nm</p> | <p style="text-align: center;">10^0-10^2 nm</p> |
| $P = v/a_0l$ | $P < 1/3$ | $1/3 < P < 1/2$ | $1/2 < P < 1$ | $P \sim 1$ |
| aggregates | sphere | worm | vesicle | bilayer |

Figure 2 Packing parameter and corresponding micelle structure [24, p. 2]

The efficiency of diversion is affected by the injection rate and permeability contrast. These factors have an effect on the amount of calcium ions present for viscosification of the SDA [16].

2.2 Breaker Application in the Petroleum Industry

According to Al-Mutawa et al. [14], VES acid diverters are zero damaging fluids in oil wells; but core experiments show that that is not the case [25], [26].

Yu et al. [26] determined the amount of VES retained in the core in order to quantify the extent of core damage done by the VES. They injected VES-acid solution at a rate of 1.5 cm³/min in order to fully retain the VES in the core. After injecting 1.8 pore volumes of VES-acid, they injected 2.8 pore volumes of the 10 vol % mutual solvent, which is a breaker, in the reverse direction. The amount of VES retained in the core after the injection of mutual solvent was 78.8%. They concluded that internal breakers are needed to break the VES gel.

Huang and Crews [8], [25] determined how efficiently hydrocarbons will reduce VES gel viscosity only by reservoir flow in both matrix acidizing and hydraulic fracturing applications. When internal breakers were not used, the initial flowback pressure needed to flow through the core was very high. This was not the case after using an internal breaker [8], [25]. Moreover, some hydrocarbons did not reduce VES viscosity by mere contact but required high energy mixing. Thus, Huang and Crews stated that VES gels might kill a well located in a low-pressure gas reservoir [25]. In a case study, the permeability recovery after flowing nitrogen gas was 2 % when internal breakers were not used, compared to over 100 % when an internal breaker was used. When testing for

the conductivity recovery of proppants, a 100 % recovery was achieved when internal breakers were used, whereas an 80 % recovery was achieved without using an internal breaker [8].

Different types of breakers have been patented in the petroleum industry [27]–[35]. Each breaker has its own VES system and conditions in which it is highly efficient.

2.3 Experimental Details and Proposed Breaking Mechanisms

Lin and Eads [36] studied the effect of polyethylene glycol (PEG) and polypropylene glycol (PPG) on oleate soap surfactant solution at room temperature. Two types of PEG were used: PEG-4600 and PEG-8000. PEG-4600 was used only for nuclear magnetic resonance (NMR). Rheology and NMR confirmed the reduction of viscosity by both polymers. Cryo-TEM was used to determine the shape of the micelles. Threadlike micelles were present after adding 1% PPG while spherical micelles were formed after adding 1% PEG. Thus, PEG was more efficient than PPG at the same concentration. They concluded that molecular mass did not affect breaking capacity in their case. They also concluded that hydrophobicity was not the only factor that affected the change of micelles in oleate soap solution from cylindrical to spherical, unlike earlier experiments that reported that hydrophobicity affected the strength of the breaker.

Sato et al. [37] studied the effect of decane on a surfactant system solution composed of monohexadecanoate ($C_{16}SE$) and monocaprylin (MG-8) using rheology and small angle x-ray scattering (SAXS). Rheology was conducted at 30°C. The surfactant system concentration was 20 %, with MG-8 weight fraction fixed at 0.05. Increasing decane concentrations reduced the viscosity of the surfactant system (~73 Pa.s to ~0.3 Pa.s).

SAXS confirmed the production of spherical micelles after the addition of decane. They explained the reduction of viscosity of the surfactant system to be due to decane solubilization in the micellar core.

Molchanov et al. [38] studied the effect of n-dodecane and n-heptane on potassium oleate surfactant solution at 20°C. Rheology and small angle neutron scattering (SANS) were used for the study. High concentrations of the hydrocarbons reduced the viscosity (from ~ 350 Pa.s to $\sim 1 \times 10^{-3}$ Pa.s) a day after sample preparation. The trend produced by the resulting mixture after SANS measurements was characteristic of spherical micelles. They proposed that the micelles underwent a change in size that affected the molecular packing parameter. This change in size was due to the solubilization of the non-polar oil in the cylindrical micelle core. The spherical micelles were formed the moment the value of the molecular packing parameter of a spherical micelle was attained.

Kumar et al. [39] studied the effect of the organic salts sodium hydroxynaphthalene carboxylate (NaHNC) and sodium salicylate (NaSal) on the amphoteric surfactant erucyl dimethyl amidopropyl betaine (EDAB) at room temperature using rheology. Both salts reduced the viscosity of the VES solution from infinite viscosity to approximately 1×10^3 Pa.s. NaHNC reduced the viscosity of the VES solution at lower concentrations than NaSal. They explained the reduction of viscosity of EDAB by organic salts by comparing the same effect of these salts on a cationic VES. The viscosity of cationic VES solutions increases in the presence of these salts due to the presence of the negative ions binding to the cationic part of the VES. The researchers proposed that the negative ions of these salts bind on the cationic part of the zwitterionic VES, but with a different effect to that of cationic VES. With the anionic part of the salt bound on EDAB, EDAB was changed

into an anionic VES that led to a change from cylindrical to spherical micelles. But, they emphasized that the binding is due to hydrophobic interactions and not to electrostatic interactions; the electrostatic interactions in EDAB are very weak due to the presence of weak charges. They also concluded that hydrophobicity affected the magnitude of viscosity reduction. NaHNC is more hydrophobic than NaSal. The higher hydrophobic salt reduced the viscosity of VES solution at a lesser concentration than the lower hydrophobic salt.

Sharma et al. [40] tested the effect of two fluorinated oils at 25°C on a non-ionic fluorocarbon surfactant system solution. The surfactant system was composed of two surfactants that belong to one class: perfluoroalkyl sulfonamide ethoxylate, $(C_8F_{17}SO_2N(C_3H_7)(C_2H_4O)_nH$, also written as $C_8F_{17}EO_n$), where n differentiates the surfactant. The surfactants used in their study had values of $n = 20$, and $n = 3$. The breakers used were the following fluorinated oils: perfluoropolyether ($F-(CF_2CF_2CF_2O)_n-CF_2CF_2COOH$ or $(C_3F_6O)_nCOOH$) and perfluorodecalin ($C_{10}F_{18}$). The value of n for the perfluoropolyether used was 21. Perfluoropolyether is amphiphilic while perfluorodecalin is hydrophobic. Rheology and SAXS were used for the study. Increasing perfluoropolyether concentrations continuously reduced the viscosity of the VES solution with increasing concentration until phase separation was achieved. Perfluorodecalin reduced the viscosity with increasing concentration until there was no further viscosity reduction. The viscosity at this plateau was higher than the minimum viscosity reached by perfluoropolyether. From SAXS, a trend characteristic of the presence of spherical micelles was reported in the case of perfluoropolyether, while a trend characteristic of cylindrical micelles was reported in the case of perfluorodecalin. The reduction in

viscosity in the presence of perfluorodecalin was due to the reduction in the size of the cylindrical micelles. They proposed that the non-polar part of perfluoropolyether created an oil pool in the micellar core while the polar part came close to the hydrophilic/hydrophobic interface of the surfactant. The oil pool formation is linked to its long oil chain. This changed the cylindrical micelle to a spherical micelle. The proposed explanation for the effect of perfluorodecalin was that it only solubilized near the hydrophobic core of the micelle, making it less efficient than perfluoropolyether.

Shibaev et al. [18] studied how n-dodecane changed the micelles in potassium oleate solutions from a cylindrical shape to a spherical shape at room temperature. The methods they used for the study were rheology, SANS, and dynamic light scattering (DLS). They identified three stages of micelle change. The first stage was the micellar network regime in which the VES retained its viscoelastic properties, despite the reduction in viscosity. The second stage was the transition stage in which the viscosity reduced drastically with increasing n-dodecane concentration because of the continuous reduction of micelle length, and the formation of microemulsions. The last stage was the microemulsion regime in which the viscosity of the solution became close to that of water and fully composed of microemulsions larger than a fully extended surfactant tail. They considered the reduction of viscosity in the micellar regime to be due to the shortening of potassium oleate cylindrical micelles after the solubilization of n-dodecane in the micelle core. They pointed out that solubilization in the end caps of the micelles was preferred to solubilization in the cylindrical section. The sharp viscosity reduction in the transition regime was due to the formation of microemulsions and the shortening of cylindrical

micelles. The microemulsion regime occurred after all the cylindrical micelles were transformed into microemulsions.

Sullivan et al. [34] proposed that the hydrophobic region of globular proteins such as alpha-amylase contributed to viscosity reduction of a VES gel at 65.6°C-121°C. The VES system they used comprised of 38 wt % erucylamidopropyl dimethyl betaine, 1.1 wt % polynaphthalene sulfonate, 22 wt % isopropanol, 5 wt % sodium chloride and 33.9 wt % water. The hydrophobic region of these proteins is inward while the hydrophilic region is outward at room temperature. An increase in temperature exposed the hydrophobic region of the protein that led to a reduction in viscosity of the VES.

Crews and Huang [30] proposed the “pin-hole effect” when both unsaturated fatty acid and mineral oil were used together as breakers at 57°C and 105°C. They used an amine oxide surfactant solution for the study. The unsaturated fatty acid underwent oxidization and dispersed in the VES micelles. This dispersion weakened the thermodynamic energy between the headgroups of the micelles, water, and counterions, allowing the mineral oils to associate with the rest of the micelles.

Sullivan et al. [35] proposed that micelle structures were destroyed by a degradable acid like PGA at 66°C that reduced the viscosity of a VES gel. The VES system they used consisted of 40 wt % EDAB, and 60 wt % water, sodium chloride, and isopropanol. About 1 wt % of low molecular weight sodium polynaphthalene sulfonate was added to the VES system.

Two solubilization mechanisms of oils by micelles have been proposed. One mechanism is the surface reaction mechanism in which the surfactant micelle temporarily adsorbs at

the oil-water interface and take in oil molecules [41]. This mechanism was proposed for non-polar oils such as triglycerides [42]. The second mechanism is the bulk reaction mechanism, in which surfactant micelles can capture polar oil molecules dissolved in aqueous solution [41]. Both mechanisms can occur if the oils have a marginal solubility in water [42]. Todorov and co-workers experimentally verified the surface reaction mechanism for cylindrical micelles solubilizing triglycerides [43].

The most extensive work done so far in describing the mechanism of viscosity reduction by breakers was by Shibaev and coworkers [18]. But their work considered only room temperature, whereas VES solutions are used at temperatures greater than 25°C in the oilfield. Siriawatwechakul and coworkers [44] developed a solvent/temperature superposition formula to predict the behavior of micelles with organic compounds at high temperatures. But they did not describe any mechanism for viscosity reduction at high temperatures. The studies conducted at high temperatures were not extensive as the study from Shibaev and coworkers [18]. Thus, this work will address how the viscosity of a long-tail VES solution is reduced at low and high temperatures by organic compounds.

CHAPTER 3

THEORITICAL BACKGROUND

3.1 Rheology

Rheology is the study of deformation and flow of matter, and delineating the relationships between stress and deformation of materials [45, p. 1]. It can either be steady shear rheology or dynamic shear rheology [38]. Steady shear rheology involves measuring viscosity at different shear rates when steady state flow has been reached [38]. Dynamic shear rheology involves measuring the behavior of materials under increasing stress or strain at different oscillation frequencies [5], [38]. The rheological parameters of interest when studying VES solutions are zero-shear viscosity (η_0), storage modulus (G'), loss modulus (G''), relaxation time (τ_R), and complex viscosity(η^*).

Zero-shear viscosity is the viscosity of the fluid when it is not sheared. It is obtained from steady or dynamic shear rheology [40]. Storage modulus gives information on how much energy can be stored in a fluid while loss modulus shows how much energy is lost as heat by the fluid [45, p. 54]. They are obtained from dynamic shear rheology and are useful in measuring the viscoelasticity of any material [5]. When oscillatory deformations are used, the difference in phase angle between the stress and strain will determine G' , G'' and η^* [5]. This phase difference determines whether a material is elastic, viscous or viscoelastic [46].

3.1.1 Theory of Maxwellian Fluids

Viscoelastic fluid behavior can be modeled using the Maxwellian model. Maxwellian fluids follow the following relations:

$$\eta_0 = G_0 \tau_R \quad (2)$$

$$\tau_R = \frac{1}{\omega_c} \quad (3)$$

$$G' = \frac{G_0 (\tau_R \omega)^2}{1 + (\tau_R \omega)^2} \quad (4)$$

$$G'' = \frac{G_0 (\tau_R \omega)}{1 + (\tau_R \omega)^2} \quad (5)$$

where η_0 is the zero-shear viscosity, G_0 is the plateau modulus, τ_R is the relaxation time, ω_c is the crossover frequency (the frequency at which G' is equal to G''), and ω is the angular frequency. Viscoelastic fluids behave as Newtonian fluids at low shear rates and shear-thinning fluids at high shear rates. Zero-shear viscosity is extrapolated from the Newtonian region at low shear rates from the viscosity versus shear rate plot. Relaxation time represents the time it takes for a Maxwellian fluid to release stress after mechanical forces are removed [47, p. 429]. G_0 is the storage modulus at high angular frequencies. For Maxwellian fluids, the plot of G'' vs G' is a semi-circle. This plot is known as the Cole-Cole plot.

3.1.2 Theory of viscoelastic surfactants rheology

VES solutions form cylindrical micelles at high concentrations. The ends of each cylindrical micelle have a semi-spherical shape. According to Cates and Candau [48], the average contour length of a cylindrical micelle, \bar{L} , is related to surfactant volume fraction, c , by the following equation

$$\bar{L} \cong c^{1/2} \exp\left(\frac{E_{sciss}}{2k_b T}\right) \quad (6)$$

where k_b is the Boltzmann constant, T is the temperature in K , and E_{sciss} is the scission energy of a micelle. This is the energy needed to break a micelle into two and form two new hemispherical endcaps.

Cylindrical micelles break and reform, and also reptate (the slithering motion of cylindrical micelles). When breaking time, τ_{br} , is smaller than reptation time, τ_{rep} , VES fluids act as Maxwellian fluids with one single relaxation time [48], given by the relation

$$\tau_R = \sqrt{\tau_{br} \tau_{rep}} \quad (7)$$

VES deviate from Maxwellian fluid behavior at high angular frequencies. At this point, breaking time greatly exceeds reptation time. This leads to the existence of a local minimum of G'' , G''_{min} [49], representing a deviation from Maxwellian fluid behavior.

Cates and coworkers [48], [49] derived the following relationship between micelle mesh size, ξ , micelle persistence length, l_p , micelle entanglement length, l_e , and plateau modulus

$$G_0 \cong \frac{(k_b T)}{\xi^3} = \frac{k_b T}{\frac{9}{6} \frac{l_e^5 l_p^5}}{\quad} \quad (8)$$

Persistence length represents the length of a micelle at which a micelle is considered inflexible while entanglement length is the micelle contour length between two entanglement points. Mesh size represents the density of entanglements.

Also, L is related to G_0 through the equation [49]

$$\frac{G''_{min}}{G_0} = \frac{l_e}{\bar{L}} \quad (9)$$

3.2 Cryogenic Transmission Electron Microscopy (Cryo-TEM)

This method views particles that have lengths below the wavelength of the visible light spectrum [50]. The range of particle sizes that can be viewed with this technique is 1-300 nm² [19]. This technique can differentiate between linear micelles and branched micelles [51].

Quickly vitrifying aqueous samples into thin films permits visualization at low temperatures. Humidity and temperature are controlled in a preparation chamber so as to vitrify samples at equilibrium temperature [50].

Digital cryo-TEM is a new improvement to the technique. It excludes the use of a photographic film that sometimes produces low image quality. Image quality reduction with the photographic film is as a result of the specimen attracting condensed volatile substances on its surface. Digital cryo-TEM uses charge-coupled device (CCD) cameras.

They view samples under low electron exposure, which is an advantage when viewing samples that are very sensitive to electron exposure [19].

CHAPTER 4

EXPERIMENTAL PROCEDURE

4.1 Materials

The amphoteric surfactant system was obtained from AkzoNobel, which was used without further purification. Erucamidopropyl hydroxypropyl sulfobetaine is the main surfactant reagent. Its concentration in the system is 40-45 wt %, with the rest composed of sodium gluconate, ethanol, propylene glycol, water and sodium chloride. The general structure of the surfactant is shown in Figure 3, where: (i) R^1 is a saturated or unsaturated hydrocarbon chain with 17-29 carbon atoms (ii) R^2 and R^3 are each independently selected from a straight chain or branched, alkyl or hydroxyalkyl group with 1-6 carbon atoms (iii) R^4 is either H, hydroxyl, alkyl or hydroxyalkyl group with 1-4 carbon atoms (iv) k, m and n are integers from 2-20, 1-20, and 0-20, respectively [52].

Hydrated calcium chloride ($\text{CaCl}_2 \cdot \text{H}_2\text{O}$, 99% purity) was purchased from Panreac. The organic compounds used to test for their breaking capacity were crude oil, n-decane, extra virgin olive oil (EVOO) and polyglycolic acid (PGA). N-decane (99% purity) and PGA were purchased from DuPont and Acros Organics, respectively. The structures of n-decane and PGA are shown in Figure 4 and Figure 5, respectively.

EVOO was purchased from a supermarket; it had a specific gravity of 0.907. EVOO are composed of triglyceride molecules. A triglyceride molecule is a combination of a glycerol molecule (Figure 6) and three fatty acids. The fatty acids attached to glycerol in EVOO are palmitic acid (Figure 7), stearic acid (Figure 8), oleic acid (Figure 9),

palmitoleic acid (Figure 10), linoleic acid (Figure 11), and α -linolenic acid (Figure 12). EVOO contains a mixture of the following triglycerides: (i) triglycerides in which all the fatty acids bonded to glycerol are identical, and (ii) triglycerides in which at least one of the fatty acids bonded to glycerol is different from the others [53, pp. 52–53]. Triolein is the most abundant triglyceride in EVOO [54, p. 924], and has three oleic acid units bonded to glycerol (Figure 13). The composition of fats present in the EVOO used is shown in Table 1.

Crude oil came from the Uthmaniya oil field, Saudi Arabia, and had a specific gravity of 0.897. Its composition is shown in Table 2.

4.2 Sample Preparation

Millipore deionized water was used to prepare solutions with 3.96 wt % of the surfactant system and 6.2 wt % CaCl_2 . This amount of CaCl_2 was the maximum produced from core acidizing studies [26] after comparing with other studies [26], [55]–[57]. The first step was dispersing a fixed volume of the VES in aqueous CaCl_2 solution with a disperser (T 25 digital ULTRA-TURRAX®, IKA, Germany) at 5200 rpm for at most 5 minutes. A syringe was used to take a fixed volume of the surfactant solution and mixed with varying concentrations of the organic compounds by shaking. The samples were equilibrated for a week at 30°C and 60°C in an oven. The surfactant solution phase was tested in any event of phase separation.

4.3 Rheology

Steady and dynamic shear rheology was performed at 30°C and 60°C using the Discovery Hybrid Rheometer (DHR-3) from TA Instruments. The DIN concentric cylinder geometry used had the following dimensions: cup diameter of 30.43 mm, and

bob diameter and length of 28 mm and 41.92 mm, respectively. The shear rate range used for steady shear viscosity measurements was $0.001\text{--}1000\text{ s}^{-1}$. The zero-shear viscosity was estimated using the correlations available in the rheometer software. Dynamic shear measurements were conducted within an angular frequency range of $0.1\text{--}100\text{ rads}^{-1}$ in the linear viscoelastic region of each solution. A solvent trap was used to reduce water evaporation during the measurements.

4.4 Cryo-TEM

A 50 μl droplet of the suspension was placed on a TEM copper holey carbon grid (AGAR SCIENTIFIC), and the solvent was left to dry out overnight. Secondly, a droplet of phosphotungstic acid was added as a negative stain to enhance the contrast of the organic material in the TEM images. Gel samples were also further diluted in ethyl acetate in order to obtain a clearer image from TEM observation. The TEM grids were analyzed in a Tecnai F30 microscope (FEI company), operated at 300KV, coupled with a Gatan CCD camera. Images were obtained and analyzed with the software Digital Micrograph (Gatan) in Bright Field TEM mode.

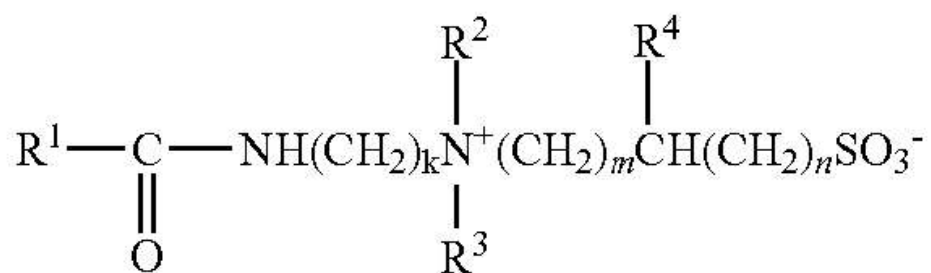


Figure 3 Chemical structure of erucamidopropyl hydroxypropyl sulfobetaine [52]



Figure 4 Chemical structure of n-decane

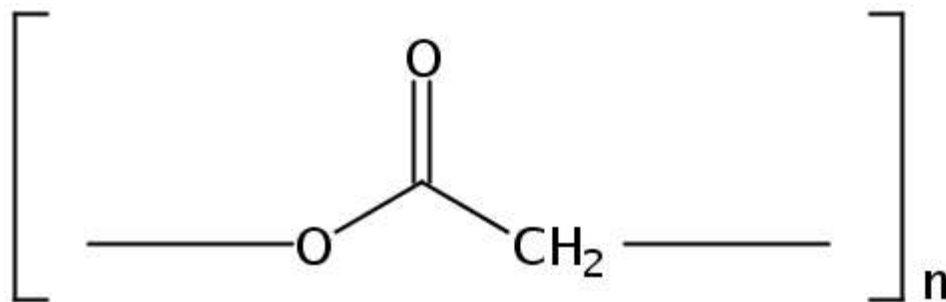


Figure 5 Chemical structure of polyglycolic acid

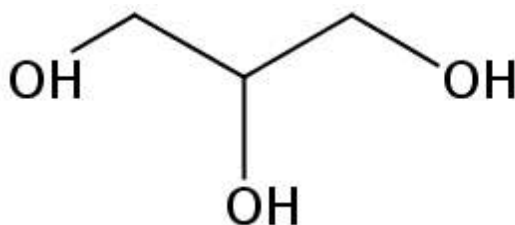


Figure 6 Chemical structure of glycerol

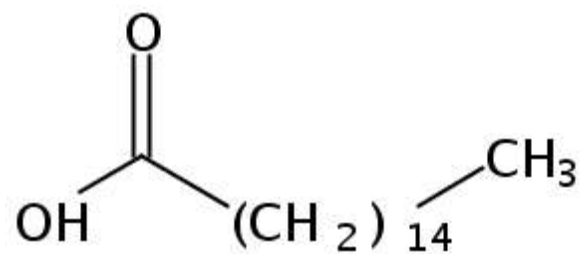


Figure 7 Chemical structure of palmitic acid

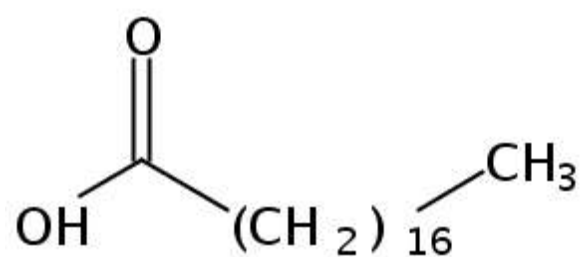


Figure 8 Chemical structure of stearic acid

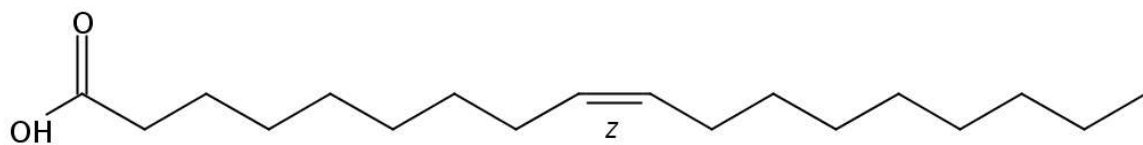


Figure 9 Chemical structure of oleic acid

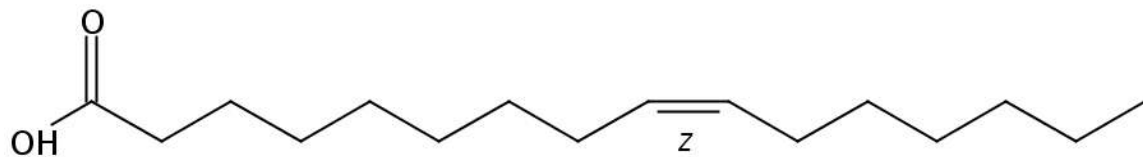


Figure 10 Chemical structure of palmitoleic acid

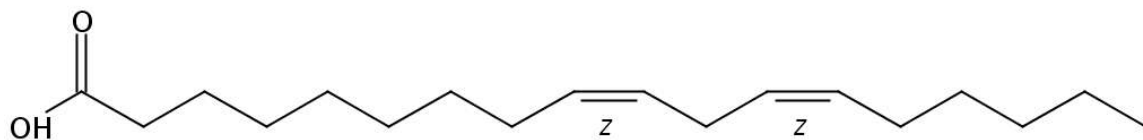


Figure 11 Chemical structure of linoleic acid

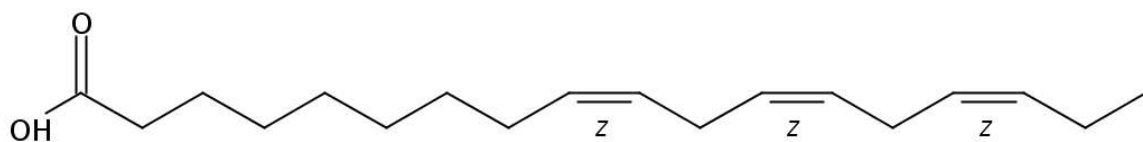


Figure 12 Chemical structure of α -linolenic acid

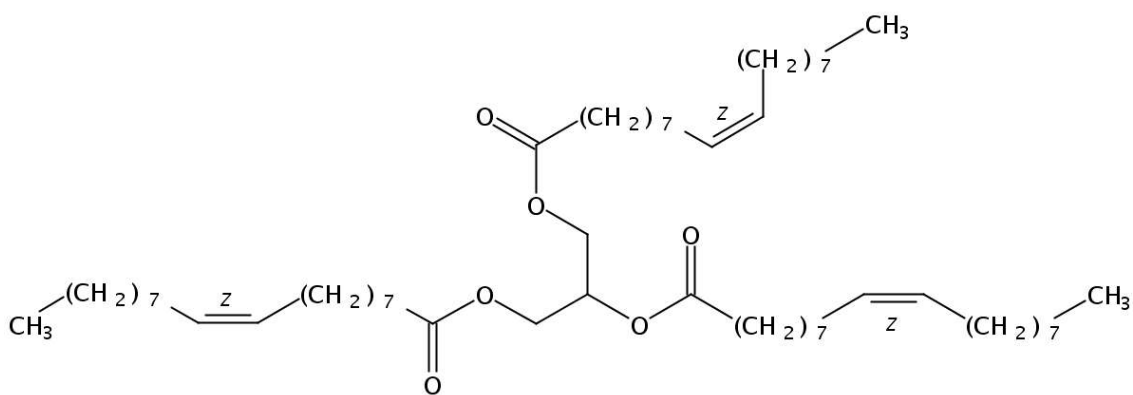


Figure 13 Chemical structure of triolein

Table 1 Extra virgin olive oil composition

| Component | Value per 100 g |
|---|-----------------|
| Saturated fats (palmitic acid, stearic acid) | 8-24 |
| Monounsaturated fats (oleic acid and palmitoleic acid) | 56-87 |
| Polyunsaturated fats (linoleic acid and α -linolenic acid) | 4-22 |

Table 2 Crude Oil composition

| Component | Moles |
|-----------|----------|
| C5 | 0.00216 |
| C6 | 0.007434 |
| C7 | 0.018767 |
| C8 | 0.027806 |
| C9 | 0.025519 |
| C10 | 0.025371 |
| C11 | 0.019607 |
| C12+ | 0.049211 |

CHAPTER 5

RESULTS AND DISCUSSIONS

This chapter is divided into two sections. The first section presents and discusses the rheological properties of the pure surfactant solution. The second section presents and discusses the effect of the organic compounds on the rheological properties of the surfactant solution.

5.1 Rheology of surfactant solution without organic compounds

The rheology of 3.96 wt % of the surfactant system solution was investigated at 30°C and 60°C. The zero-shear viscosity of the solution during the equilibration period is shown in Figure 14. Zero-shear viscosity increases with time and reaches a maximum. This indicates micellization occurred until equilibrium was reached. The following paragraphs present and discuss the results of the surfactant solution after a week of equilibration.

The plot of viscosity versus shear rate of the surfactant solution at both temperatures is shown in Figure 15. There was a transition from the Newtonian to the shear-thinning region with increasing shear rate at both temperatures. This transition is evidence that cylindrical micelles were in the surfactant solution that aligned themselves along the direction of shear flow [58], [59]. The presence of a plateau from the shear stress versus shear rate graph at 60°C during the transition (Figure 17) is evidence that a cylindrical micelle network was present in the solution [60].

There were inflection points during the transition and an apparent yield stress at 30°C as seen from the viscosity versus shear stress plot (Figure 16) and shear stress versus shear rate plot (Figure 17). High concentrations of a similar C-22 tailed sulfobetaine surfactant, 3-(*N*-erucamidopropyl-*N,N*-dimethyl ammonium) propane sulfonate (EDAS) showed similar inflection points [58], [61]. This was attributed to shear banding [58], [61]. Shear banding is the separation of a micellar solution into macroscopic regions with different shear rates [60]. Moreover, there was a sharp drop in viscosity during the transition from the Newtonian to the shear-thinning region at both temperatures as seen from the viscosity versus shear stress plot (Figure 16). Such behavior is also attributed to shear banding in micellar solutions [60]. Shear banding is due to the presence of dense micelle networks in a surfactant solution [60]. This is more evidence that dense micelle networks were present in the surfactant solution at both temperatures. Cryo-TEM revealed the presence of cylindrical micelles in the pure surfactant solution equilibrated at 30°C (Figure 19) even after being diluted in ethyl acetate (Figure 20 and Figure 21). The visibility of the inflection point at 30°C and its absence at 60°C shows that shear banding was more pronounced at the lower temperature.

From Figure 15, the zero-shear viscosity of the surfactant solution was higher at 30°C than at 60°C, though not significant (~186.1 Pa.s vs ~138.1 Pa.s, ~26 % difference). Concentrated EDAS solutions have a similar behavior [58]. The most likely reason for this difference is that the cylindrical micelle network was more entangled at 30°C than at 60°C, as cylindrical micelles close together offer more resistance to flow than micelles further apart. This is explained further when considering G' and G'' measurements of the surfactant solution.

The variation of G' and G'' of the surfactant solution with angular frequency at both test temperatures is shown in Figure 18. G' dominated G'' within the tested frequency range at both temperatures, and the crossover frequency was absent. High concentrations of the C-22 tailed amphoteric surfactants like EDAB [39], EDAS [58], and erucyldimethyl amidopropyl amine oxide (EMAO) [62] have such behavior within a frequency range of $0.01\text{-}100\text{ rads}^{-1}$ at high concentrations and low temperatures. Maxwellian fluids typically show a region in which G'' dominates G' at low angular frequencies, and a crossover frequency in which G' equals G'' . The complete dominance of G' over G'' within the angular frequency range of $0.01\text{-}100\text{ rads}^{-1}$ is attributed to gels [39]. But the existence of the Newtonian region at low shear rates (Figure 15) and G_0 (Figure 18) at both temperatures is evidence that the surfactant solution followed Maxwellian behavior at low angular frequencies and not gel-like behavior. This also implies that crossover frequencies can be estimated.

The crossover frequencies and relaxation times of the surfactant solution at both temperatures estimated from equations 2 and 3 are shown in Table 3. The estimated crossover frequencies at both temperatures were below 0.1 rads^{-1} . Thus, the crossover frequencies at both temperatures were not within the measuring frequency range. The estimated crossover frequency was lower at 30°C than at 60°C . The difference in crossover frequency at both temperatures is possibly due to the density of the entanglements at both temperatures.

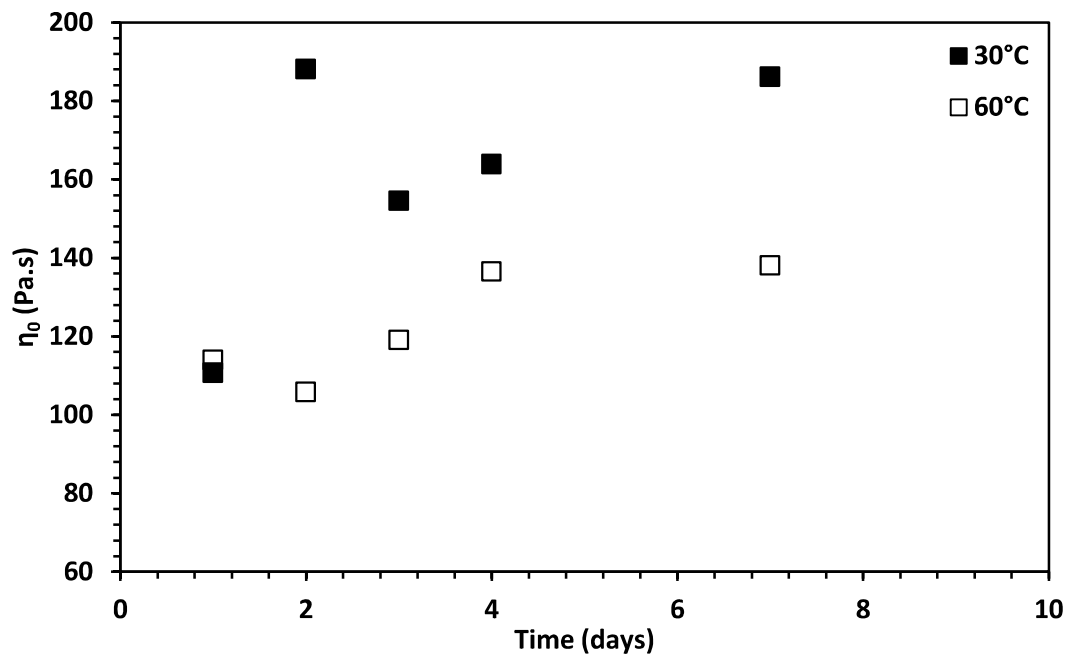


Figure 14 Zero-shear viscosity of surfactant solution with time

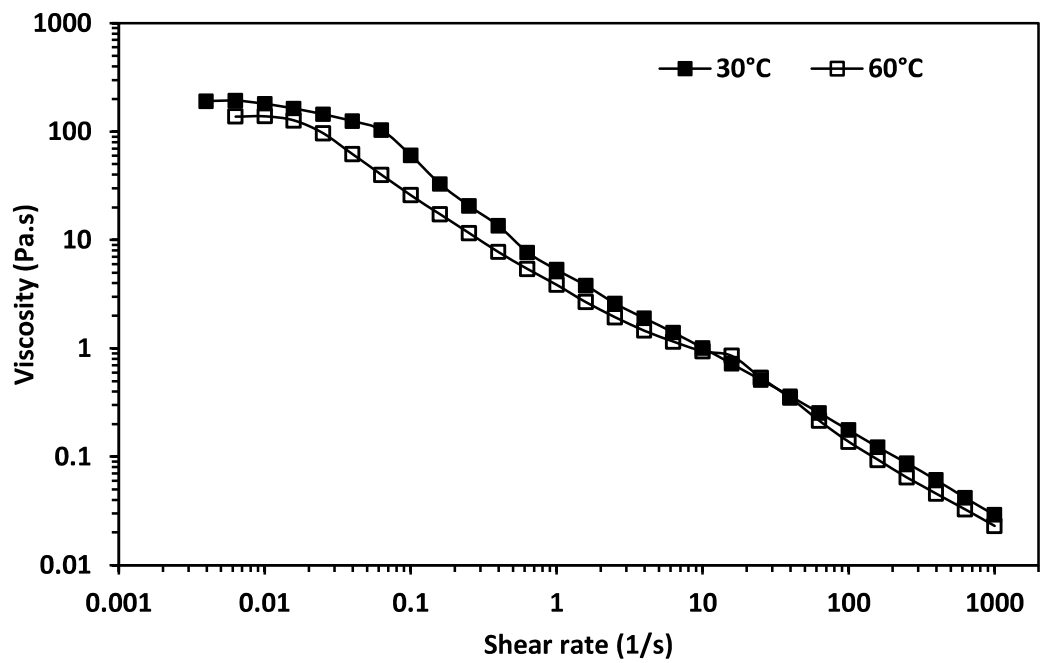


Figure 15 Viscosity vs shear rate of 3.96 wt % surfactant solution

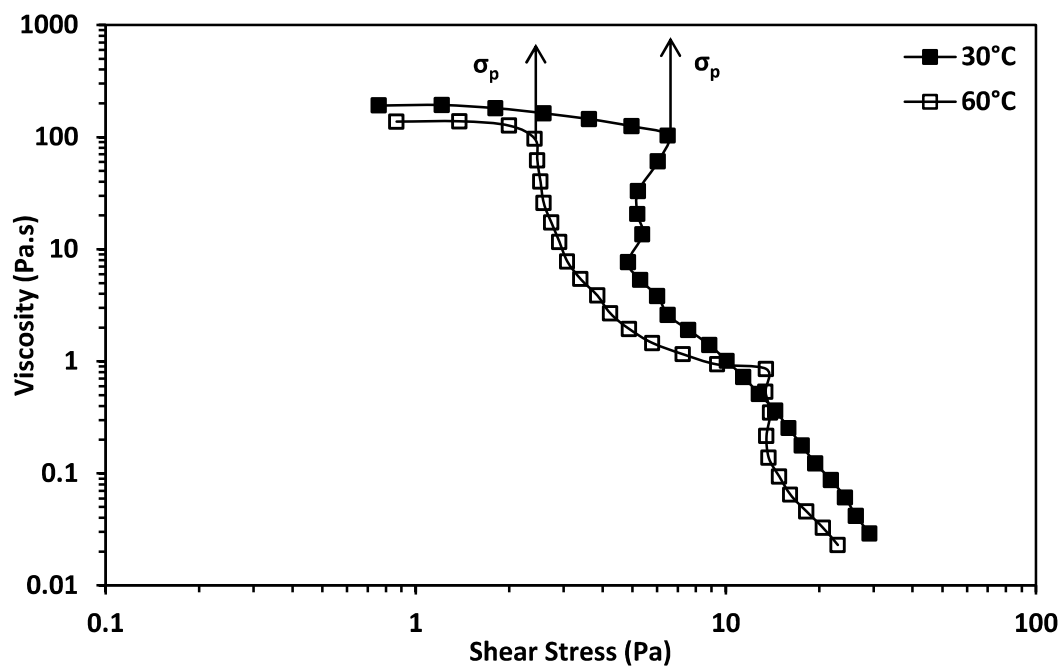


Figure 16 Viscosity vs shear stress of 3.96 wt % surfactant solution

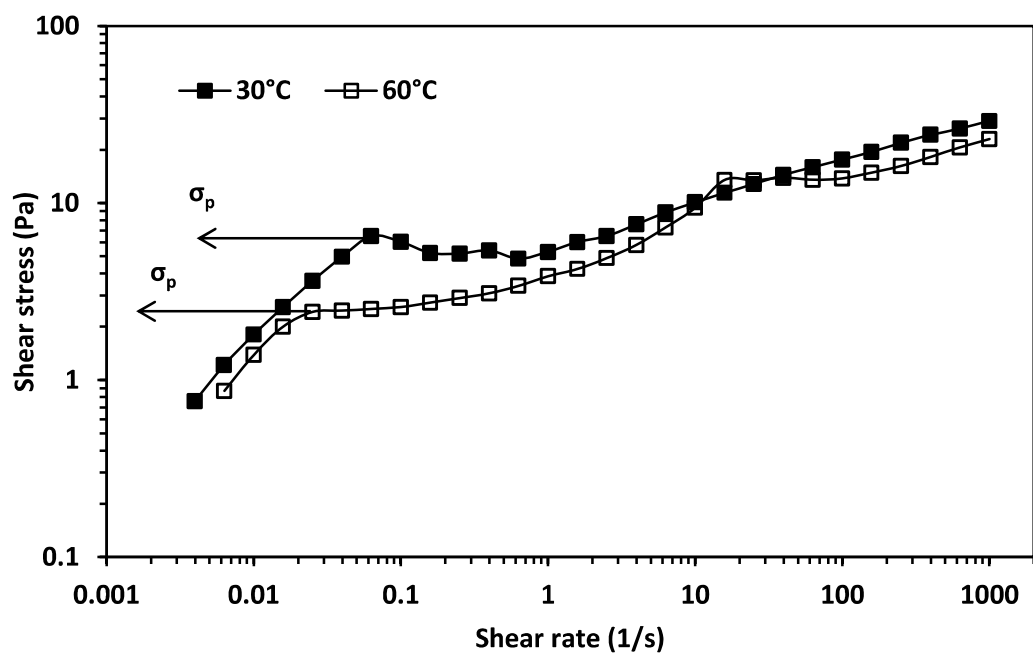


Figure 17 Shear stress vs shear rate of 3.96 wt % surfactant solution

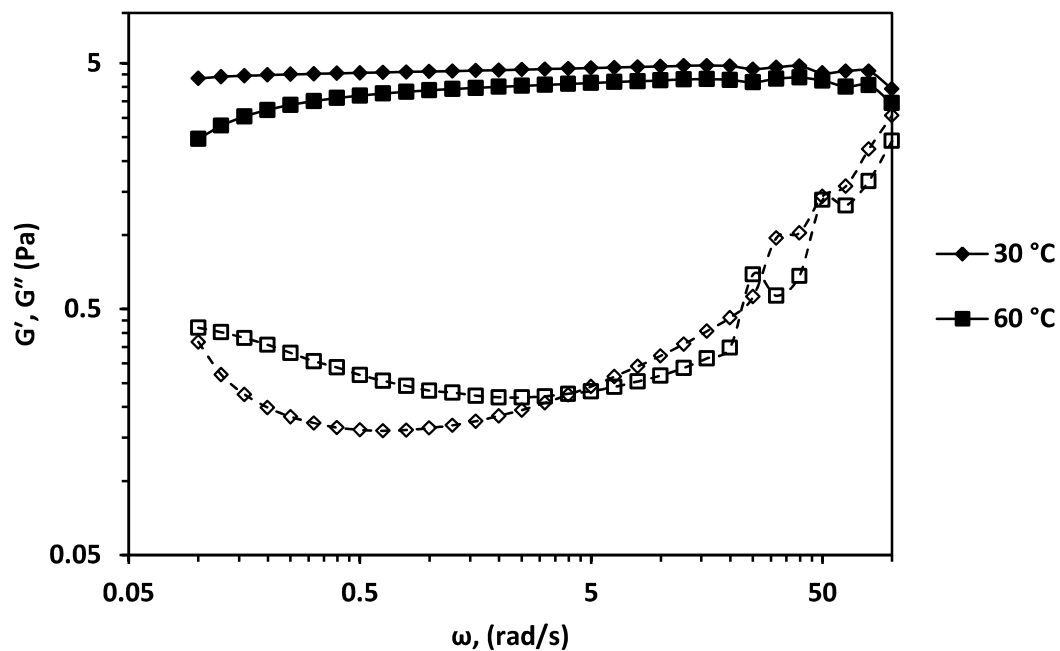


Figure 18 Storage modulus (filled symbols) and loss modulus (open symbols) of 3.96wt % surfactant solution

Table 3 Estimated values of crossover frequency and relaxation time of the pure surfactant solution

| Temperature (°C) | η_0 (Pa.s) | G_0 (Pa) | ω_c (rad/s) | τ_R (s) | ξ (nm) |
|------------------|-----------------|------------|-----------------------|--------------|------------|
| 30 | 186.09 | 4.59 | 2.47×10^{-2} | 40.5 | 97.0021 |
| 60 | 138.07 | 4.05 | 2.93×10^{-2} | 34.1 | 104.375 |

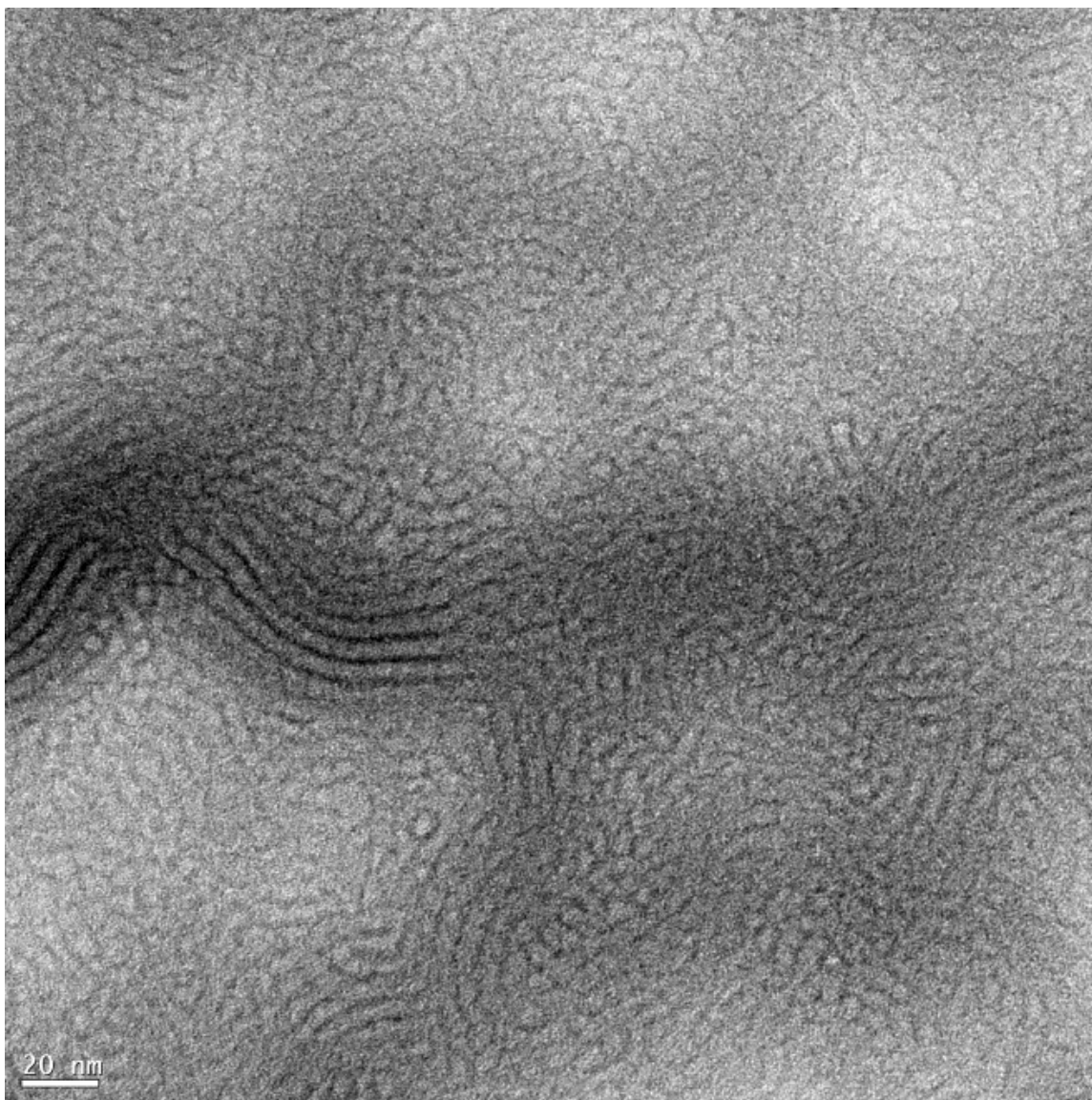


Figure 19 Cryo-TEM image of 3.96 wt % surfactant solution at 30°C. The black curves represent the edges of the micelles



Figure 20 Cryo-TEM image of 3.96 wt % surfactant solution at 30°C diluted in ethyl acetate. The black curves represent the edges of the micelles

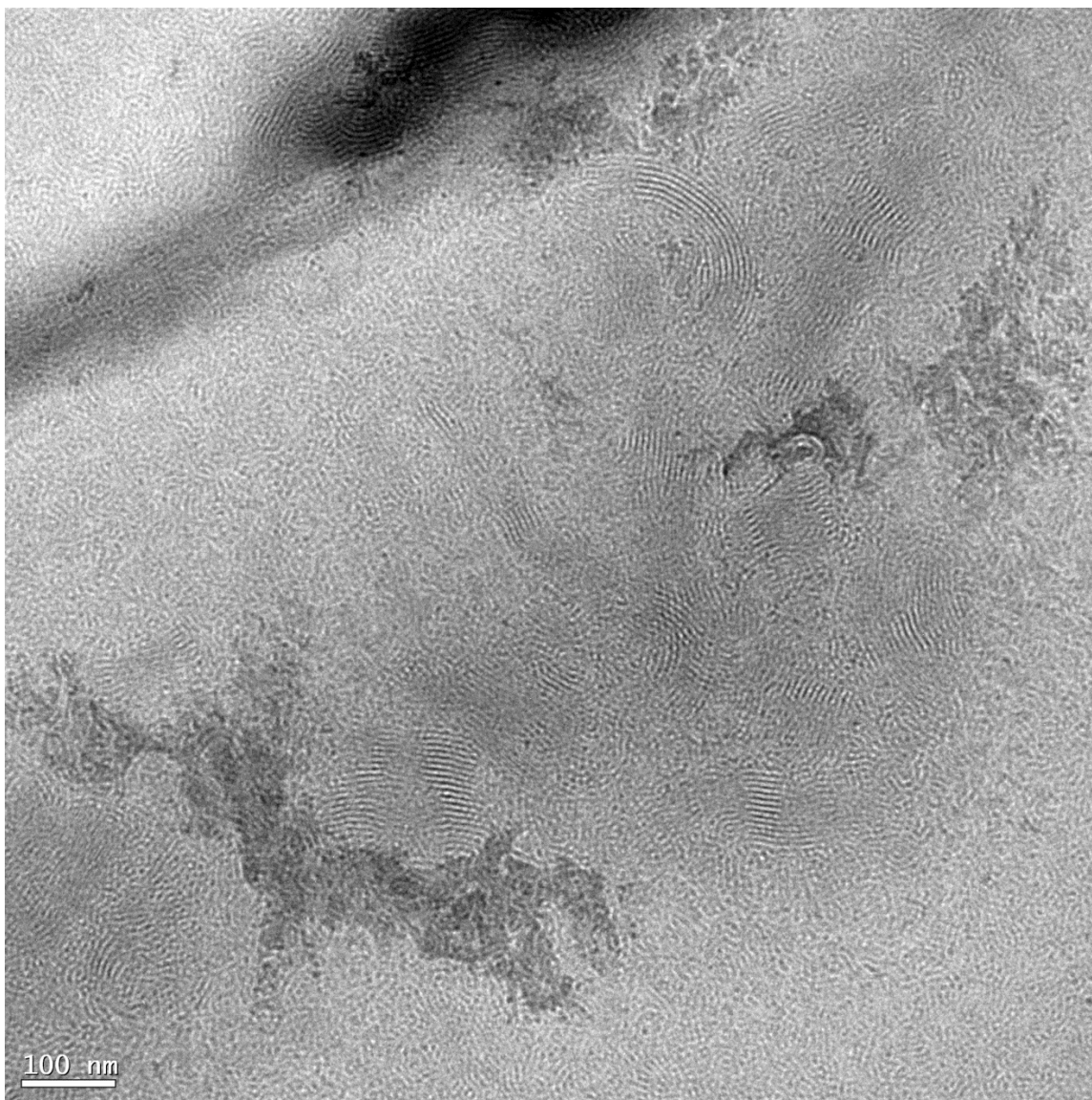


Figure 21 Cryo-TEM image of 3.96 wt % surfactant solution at 30°C diluted in ethyl acetate. The black curves represent the edges of the micelles

G''_{min} was present at both temperatures (Figure 18), meaning the solution deviated from Maxwellian fluid behavior with increasing frequency. The presence of G''_{min} and G_0 implies that ξ can be estimated using equation 8. The estimated ξ at 30°C was lower than that at 60°C as shown in Table 3. This implies the micelles were closely packed at 30°C than at 60°C. This explains why the zero-shear viscosity of the solution was higher at 30°C than at 60°C. It also explains why shear banding was more pronounced at 30°C than at 60°C.

Therefore, micellization occurred for seven days until micelle networks were formed at both temperatures.

5.2 Rheology of surfactant solution with the organic compounds

The effects of four organic compounds on 3.96 wt % of the surfactant system with 6.2 wt % CaCl_2 solution were investigated. These organic compounds were crude oil, EVOO, n-decane, and PGA. The effect of the oils and PGA at both temperatures will be presented and discussed separately.

5.2.1 Effect of the oils

The estimated zero-shear viscosity of the surfactant solution with increasing concentrations of n-decane, crude oil, and EVOO at both test temperatures are shown in Figure 22-Figure 24, respectively. The estimated zero-shear viscosities of the surfactant solution with the oils were higher at 30°C than at 60°C and reduced with increasing oil concentration.

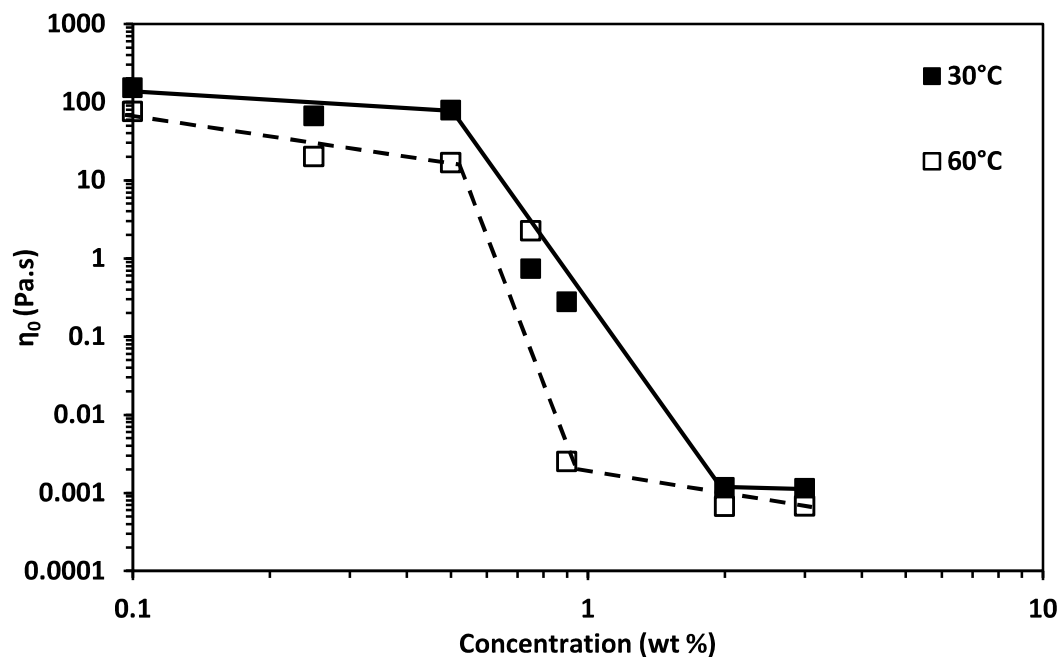


Figure 22 Estimated zero-shear viscosity of 3.96 wt % surfactant solution with different n-decane concentrations with the lines as visual aids. The full lines link the points at 30°C, whereas the dashed lines link the points at 60°C

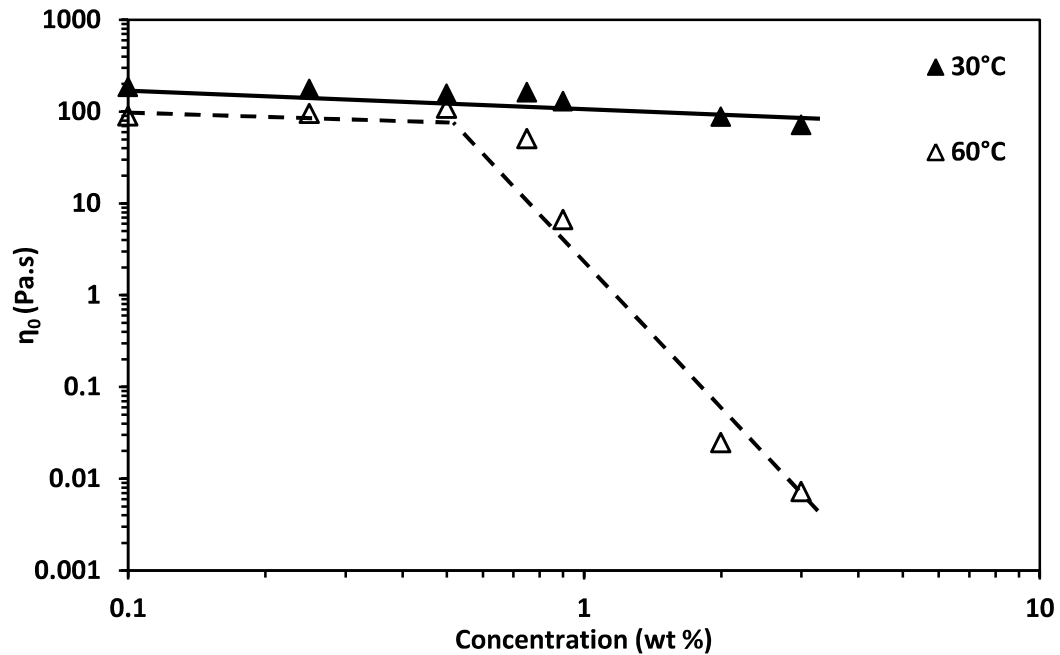


Figure 23 Estimated zero-shear viscosity of 3.96 wt % surfactant solution with different crude oil concentrations with the lines as visual aids. The full lines link the points at 30°C, whereas the dashed lines link the points at 60°C

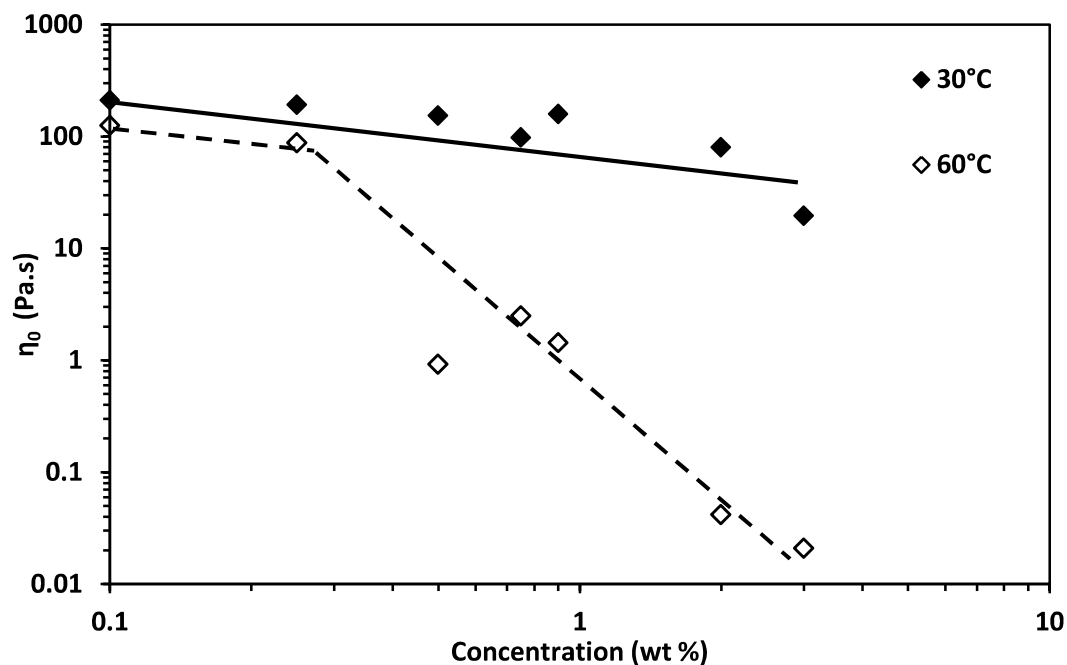


Figure 24 Estimated zero-shear viscosity of 3.96 wt % surfactant solution with different EVOO concentrations with the lines as visual aids. The full lines link the points at 30°C, whereas the dashed lines link the points at 60°C

Table 4 Estimated differences in zero-shear viscosities between the VES solutions with the oils and the pure VES solutions at test temperatures

| Concentration (wt %) | N-decane | | Crude oil | | EVOO | |
|-------------------------|--------------------|--------------------|-----------|--------------------|------|--------------------|
| | 30°C | 60°C | 30°C | 60°C | 30°C | 60°C |
| 0.9 | 6.72×10^2 | 5.50×10^4 | 1.43 | 2.08×10^1 | 1.17 | 9.65×10^1 |
| 2 | 1.58×10^5 | 2.06×10^5 | 2.12 | 5.62×10^3 | 2.33 | 3.33×10^3 |
| 3 | 1.63×10^5 | 2.05×10^5 | 2.62 | 1.92×10^4 | 9.57 | 6.59×10^3 |

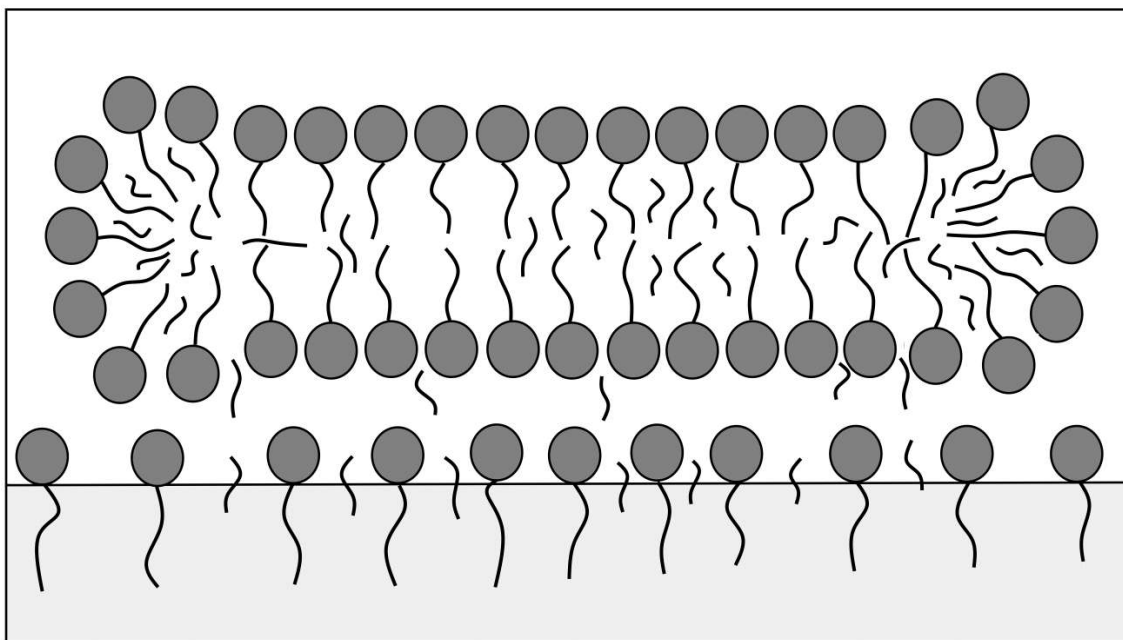


Figure 25 Schematic showing the migration of oil molecules (small strands) from an oil droplet (gray region) to a cylindrical micelle after adsorption of the micelle on the oil-aqueous solution interface

The estimated differences between the zero-shear viscosities of the surfactant solutions with the oils and the pure surfactant solutions at both test temperatures are in Table 4. At 30°C, 0.9 wt % n-decane induced a difference of approximately two orders of magnitude. Meanwhile, 0.9 wt % crude oil and EVOO induced a difference of approximately one fold. The zero-shear viscosities of the surfactant solutions with 2 wt % and 3 wt % crude oil and EVOO at 30°C were estimated to check if the effects of 0.9 wt % of these oils at this temperature were due to low concentrations. The differences induced by 3 wt% of crude oil and EVOO at 30°C were just approximately three and ten folds, respectively. Meanwhile, the surfactant solutions with 2 wt % and 3 wt % n-decane at 30°C were approximately 1 cp (Figure 22); an approximate difference of five orders of magnitude. Therefore, n-decane was more efficient than crude oil and EVOO as a breaker at 30°C.

At 60°C, 0.9 wt % of crude oil and EVOO induced a difference of approximately one order of magnitude. Moreover, 3 wt % crude oil, EVOO, and n-decane induced differences of approximately four, three, and five orders of magnitude, respectively (Table 4). Thus, increasing the temperature improved the breaking capacity of crude oil and EVOO.

Reduction of zero shear viscosity by non-polar oils is due its solubilization in the micellar core [18], [35]–[37], [39], [40], [63]. This is the only region in which non-polar oils can be solubilized as the micellar core is hydrophobic. Crude oil and EVOO faced a barrier to solubilization at 30°C which n-decane did not face. This is inferred from the insignificant differences induced by crude oil and EVOO at 30°C. Temperature reduced the effect of the barrier on crude oil and EVOO.

In order to interpret the results of this work, the solubilization kinetic model by cylindrical micelles proposed by Kralchevsky et al. [41] will be used as it has been experimentally verified [43]. Also, the fact that cylindrical micelles were formed as soon as the VES system was dissolved in aqueous solution needs to be accounted for. In this work, the most likely solubilization mechanism is the surface reaction mechanism. This mechanism is suggested because the tested oils are insoluble in aqueous solution. The schematic is shown in Figure 25. The effect of temperature can be explained thus: the temperature increased the kinetic energy of the micelles and the oil droplets. This increased the number of micelles adsorbing at the oil-aqueous solution interface to solubilize the oils, facilitating the uptake of the oil molecules into the micellar core. Moreover, the oil molecules in crude oil and EVOO had enough kinetic energy at the higher temperature to overcome the barrier to solubilization in the micellar core that existed at 30°C.

Three regimes of zero-shear viscosity change induced by n-decane can be delineated at both temperatures from Figure 22, similar to Shibaev et al. [18]: the high viscosity regime (HVR), the transition regime (TR) and the low viscosity regime (LVR). Crude oil and EVOO induced only the HVR at 30°C, and the HVR and TR at 60°C.

The high viscosity regime: The following oil concentration ranges delineated the HVR: (i) 0.1-0.5 wt % n-decane at 30°C (Figure 22), (ii) 0.1-3 wt % crude oil and EVOO at 30°C (Figure 23-Figure 24), (iii) 0.1-0.25 wt % EVOO at 60°C (Figure 24) (iv) 0.1-0.5 wt % of n-decane and crude oil (Figure 22-Figure 23) at 60°C. The surfactant solutions with the oils in this regime had high zero-shear viscosities. There were transitions from the Newtonian to shear thinning region from the steady shear rheology plots at the cited

oil concentrations at 30°C (Figure 26-Figure 28) and 60°C (Figure 29-Figure 31). Moreover, G_0 and G''_{min} were present from the dynamic shear rheology plots at the cited oil concentrations at 30°C (Figure 32-Figure 34) and 60°C (Figure 35-Figure 37). There were shear-banding transitions at these oil concentrations from shear stress versus shear rate graph (Figure 38-Figure 43). The maxima present in the viscosity against shear rate plots correspond to shear-banding transitions (Figure 44 and Figure 45). This implied that long micelles and an entangled network were present in the surfactant solutions with these oil concentrations, accounting for the high zero-shear viscosities.

Despite the absence of crossover frequencies at some oil concentrations in this regime, the surfactant solutions in this regime were Maxwellian at low angular frequencies with one relaxation time. This is because of the presence of a zero-shear viscosity and G_0 . The absence of these crossover frequencies was because they were below the measuring frequency range.

The presence of the HVR at both temperatures at these oil concentrations indicates that the oil concentrations did not prevent the formation of a micelle network during the equilibration period. The main possible reason for the existence of the HVR in the presence of n-decane at 30°C was the low n-decane concentrations. In the case of crude oil and EVOO at 30°C, few molecules in these oils had sufficient kinetic energy to penetrate the micelles. This is related to the complex molecular structure of the molecules in these oils. The different explanations for the effect of the oils at 30°C are based on the different oil concentration ranges of the HVR: the HVR existed even at 3 wt % of crude oil and EVOO, unlike n-decane in which it existed only up to 0.5 wt %.

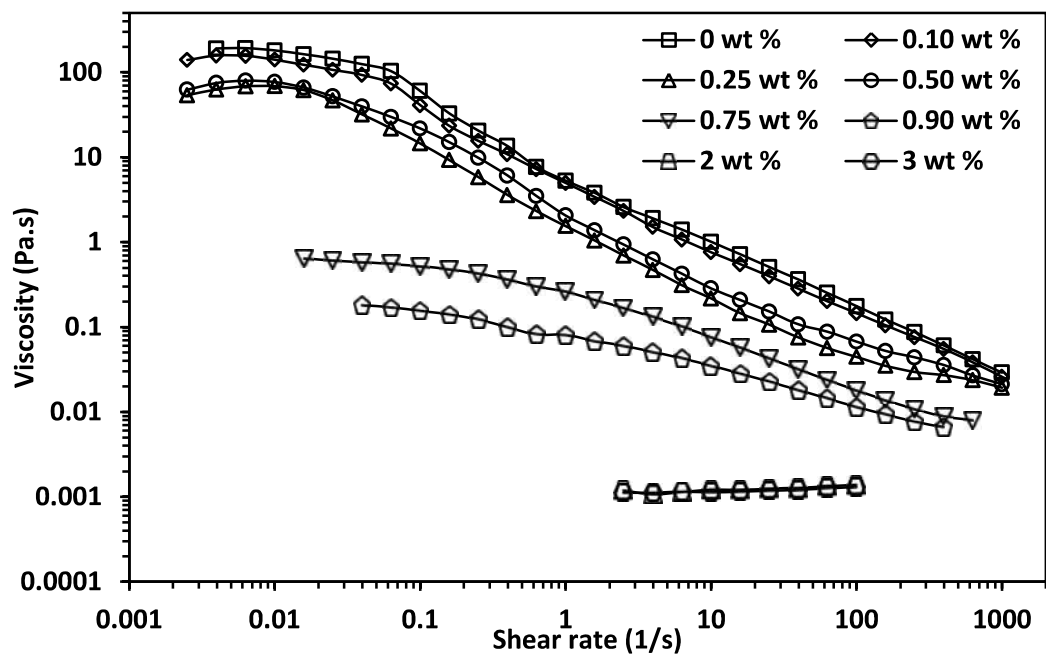


Figure 26 Viscosity vs shear rate of 3.96 wt % surfactant solution with different concentrations of n-decane at 30°C

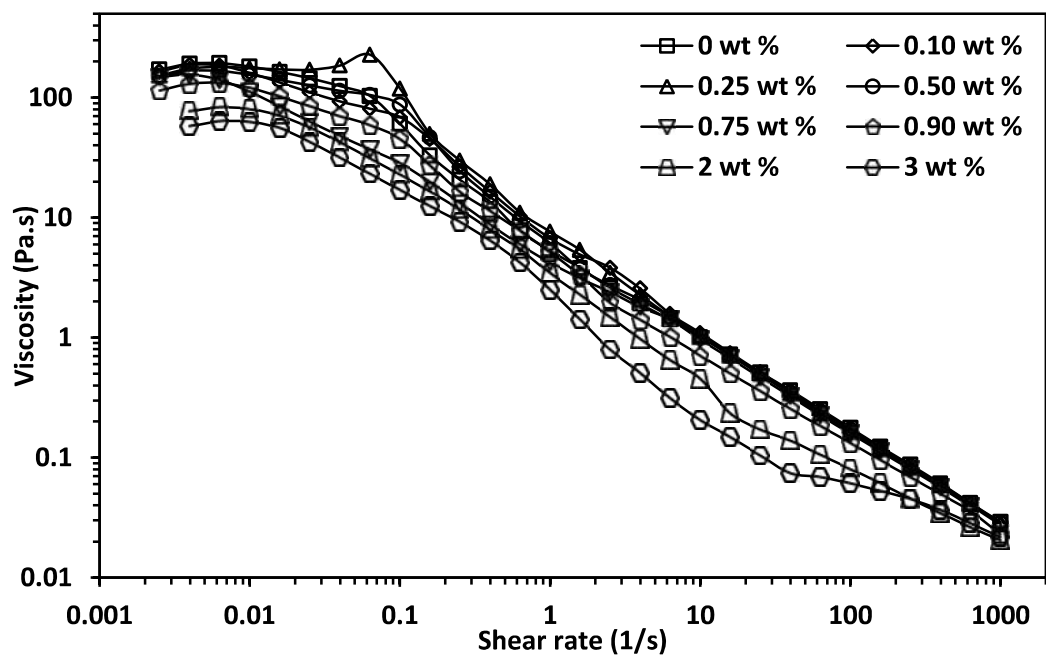


Figure 27 Viscosity vs shear rate of 3.96 wt % surfactant solution with different concentrations of crude oil at 30°C

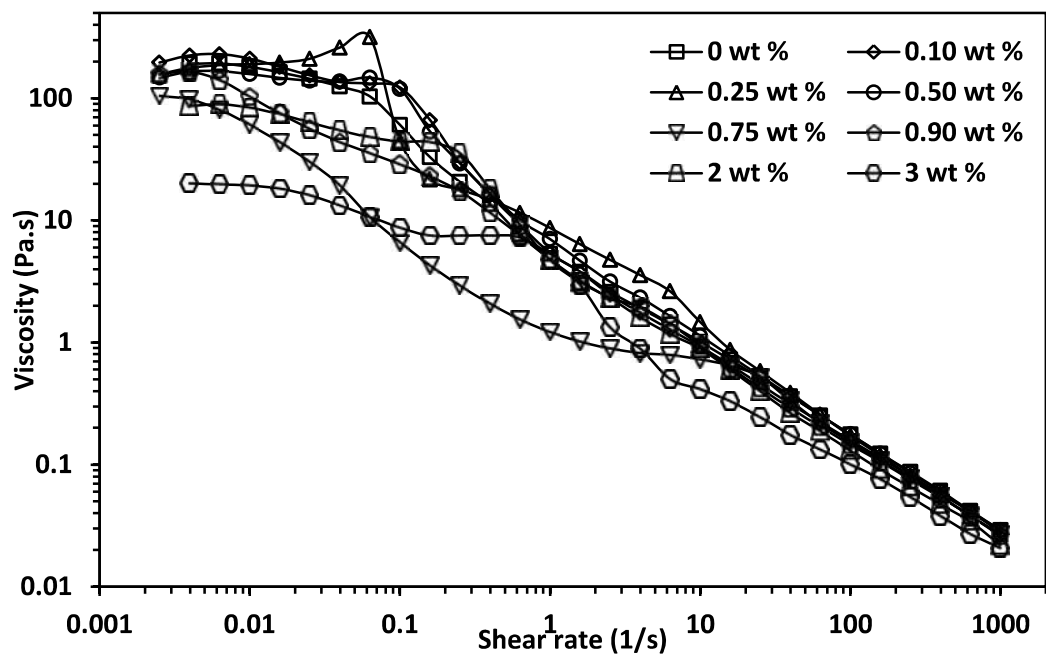


Figure 28 Viscosity vs shear rate of 3.96 wt % surfactant solution with different concentrations of EVOO at 30°C

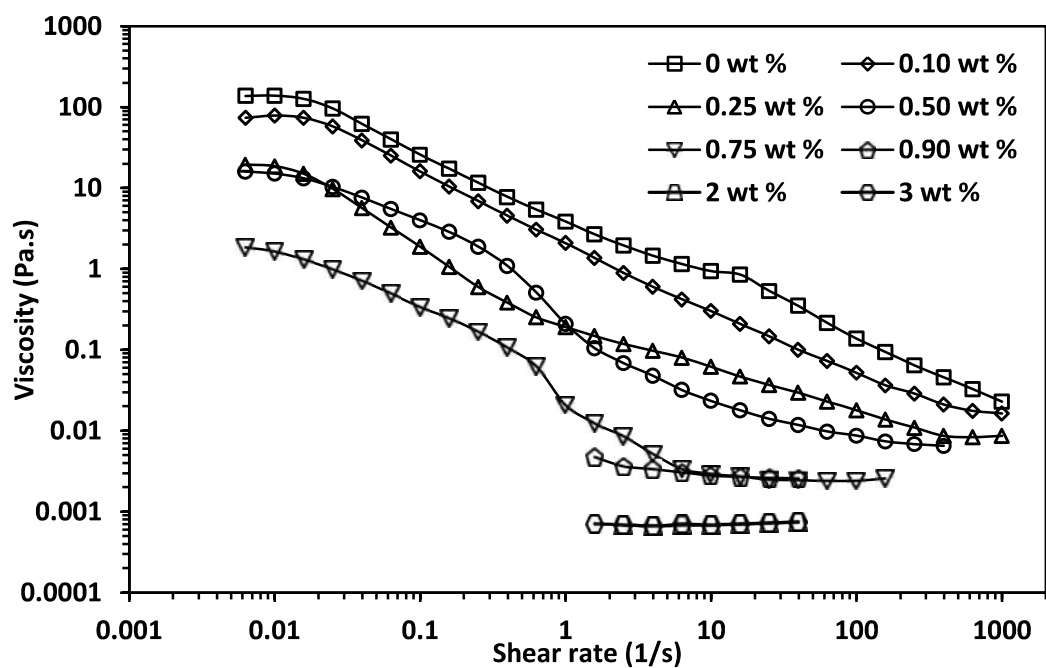


Figure 29 Viscosity vs shear rate of 3.96 wt % surfactant solution with different concentrations of n-decane at 60°C

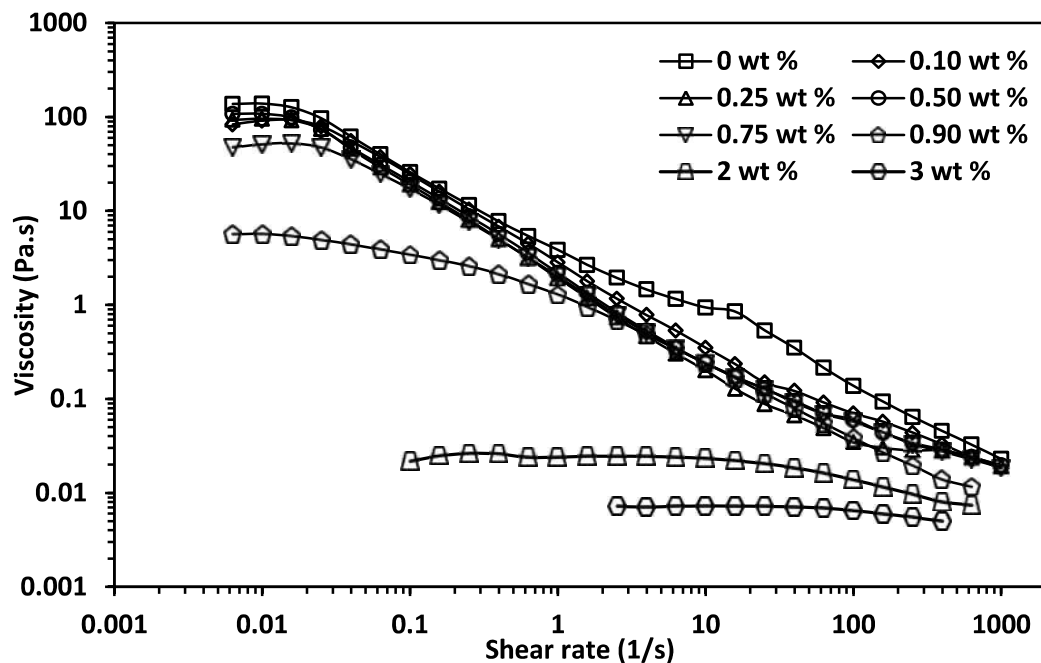


Figure 30 Viscosity vs shear rate of 3.96 wt % surfactant solution with different concentrations of crude oil at 60°C

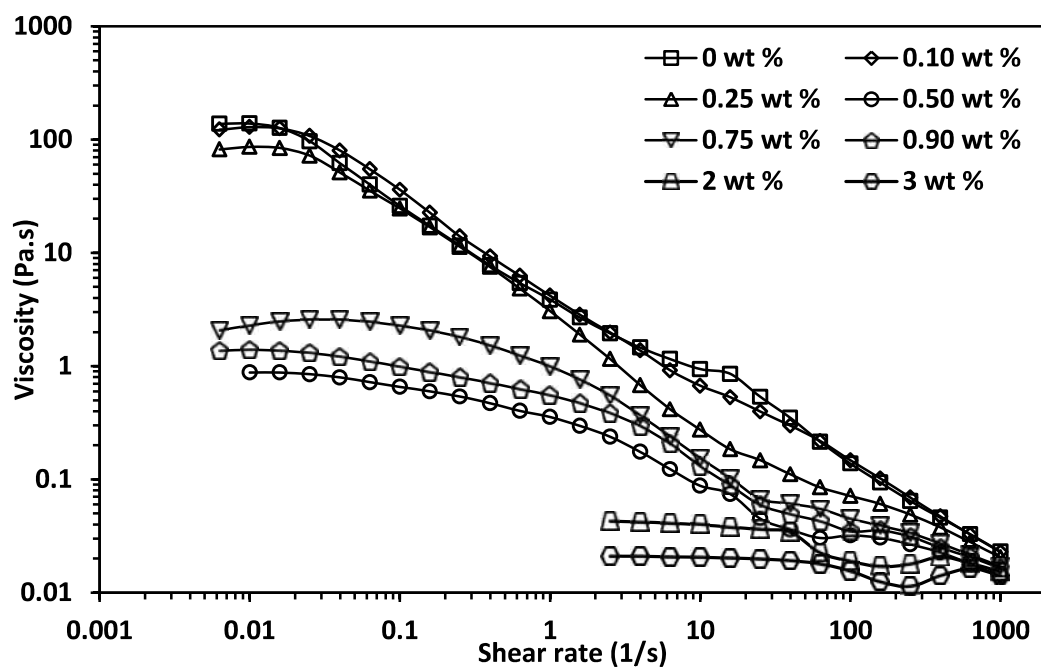


Figure 31 Viscosity vs shear rate of 3.96 wt % surfactant solution with different concentrations of EVOO at 60°C

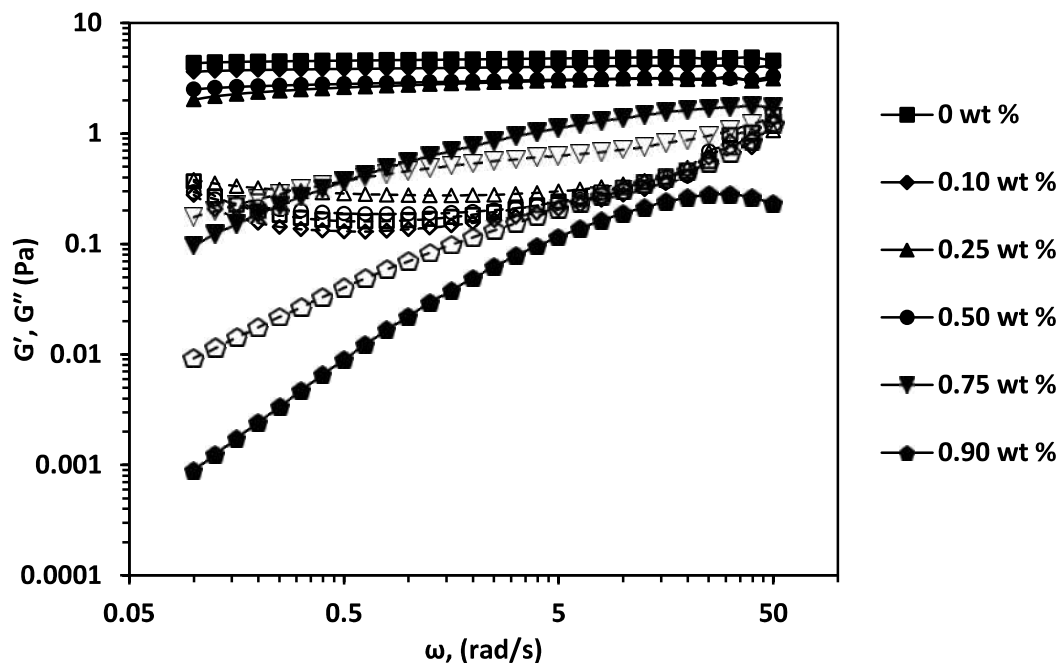


Figure 32 Storage modulus (filled symbols) and loss modulus (open symbols) of 3.96 wt % surfactant solution with different concentrations of n-decane at 30°C

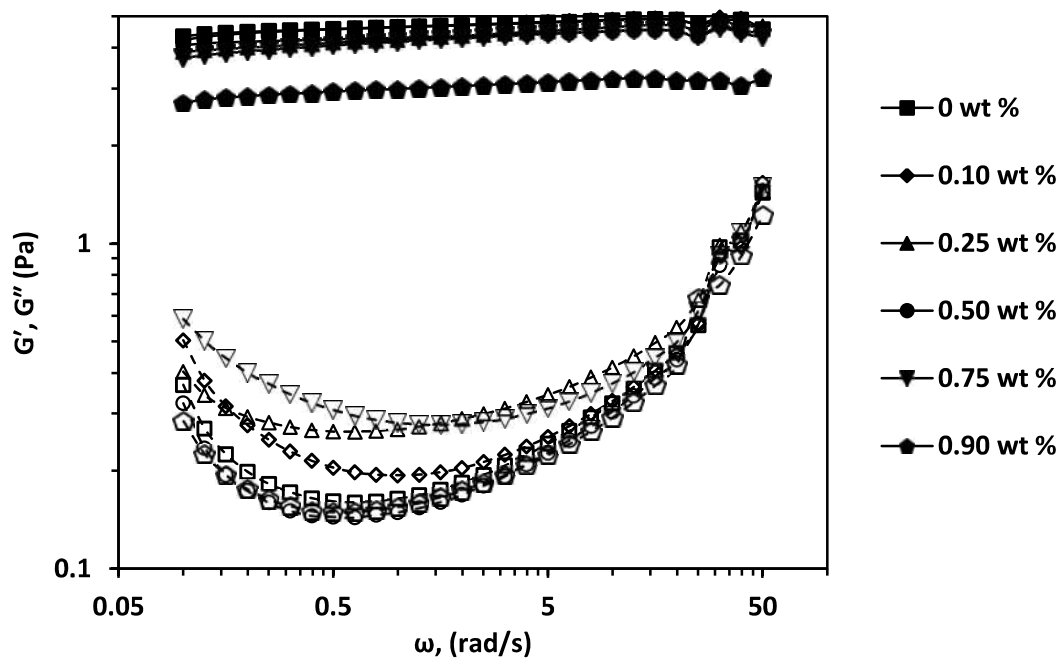


Figure 33 Storage modulus (filled symbols) and loss modulus (open symbols) of 3.96 wt % surfactant solution with different concentrations of crude oil at 30°C

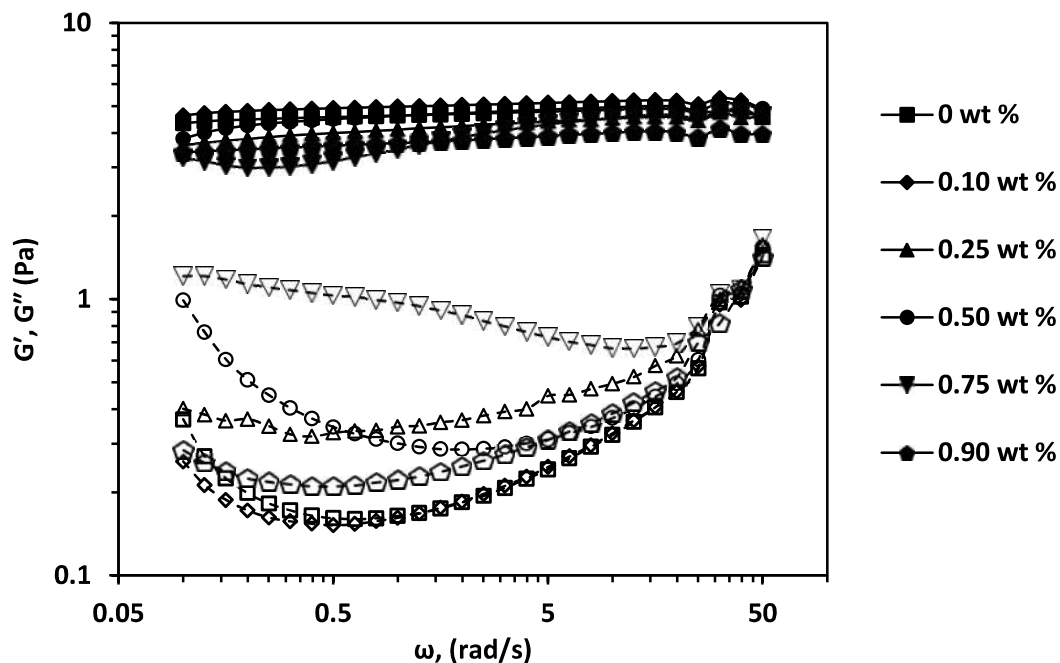


Figure 34 Storage modulus (filled symbols) and loss modulus (open symbols) of 3.96 wt % surfactant solution with different concentrations of EVOO at 30°C

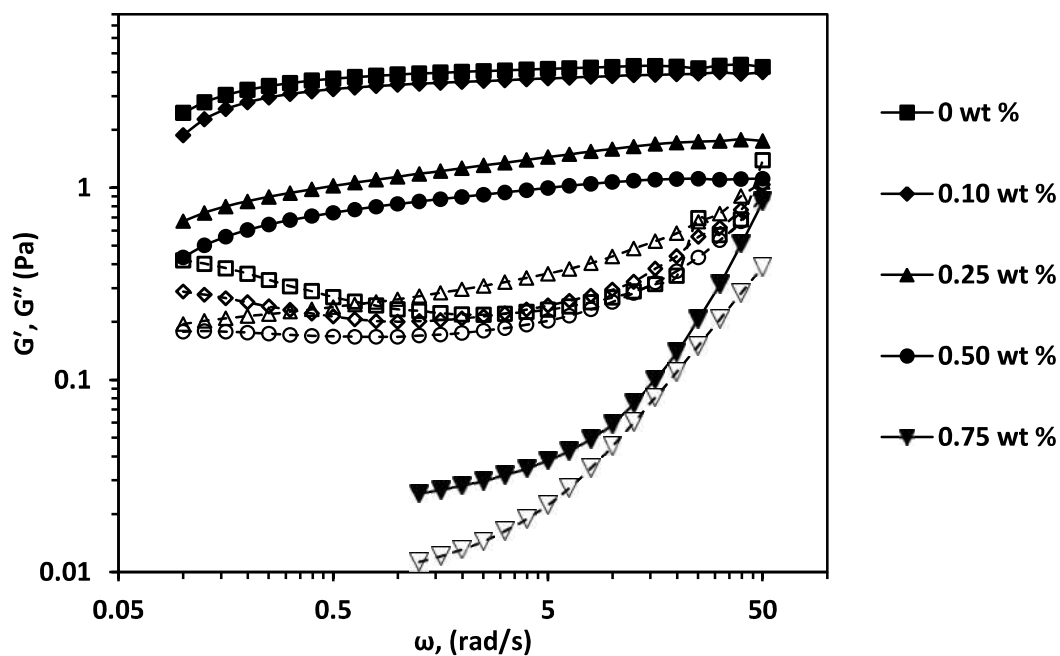


Figure 35 Storage modulus (filled symbols) and loss modulus (open symbols) of 3.96 wt % surfactant solution with different concentrations of n-decane at 60°C

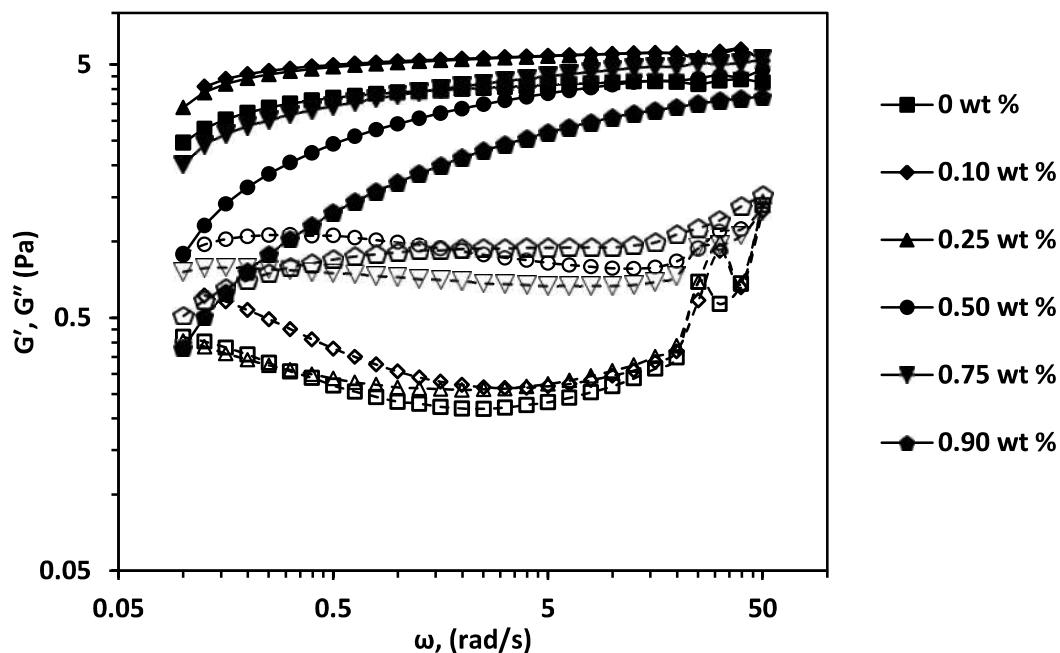


Figure 36 Storage modulus (filled symbols) and loss modulus (open symbols) of 3.96 wt % surfactant solution with different concentrations of crude oil at 60°C

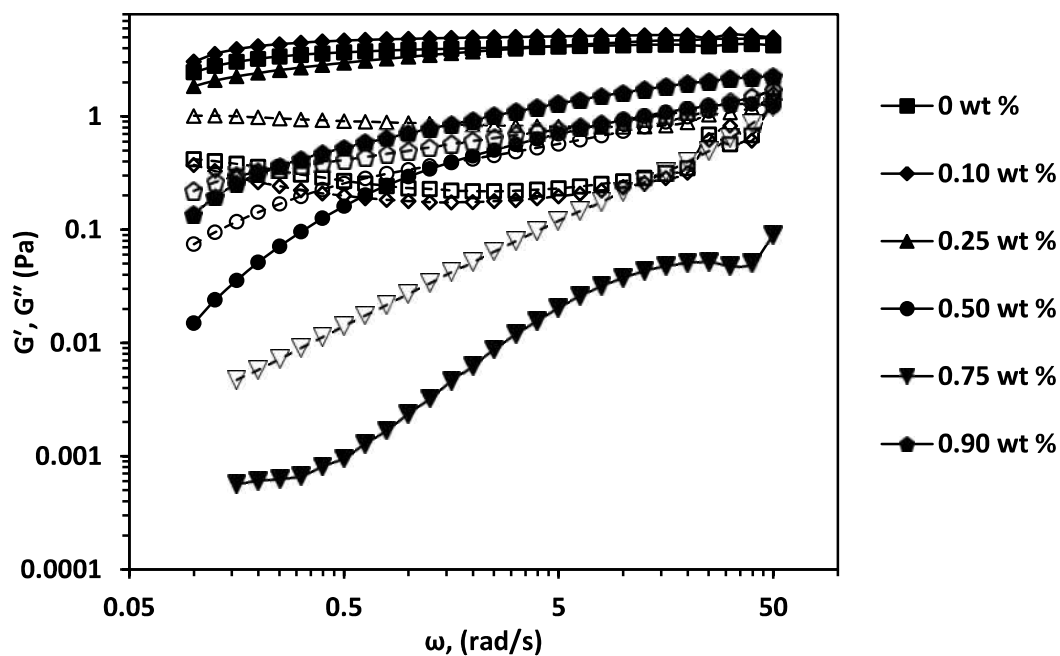


Figure 37 Storage modulus (filled symbols) and loss modulus (open symbols) of 3.96 wt % surfactant solution with different concentrations of EVOO at 60°C

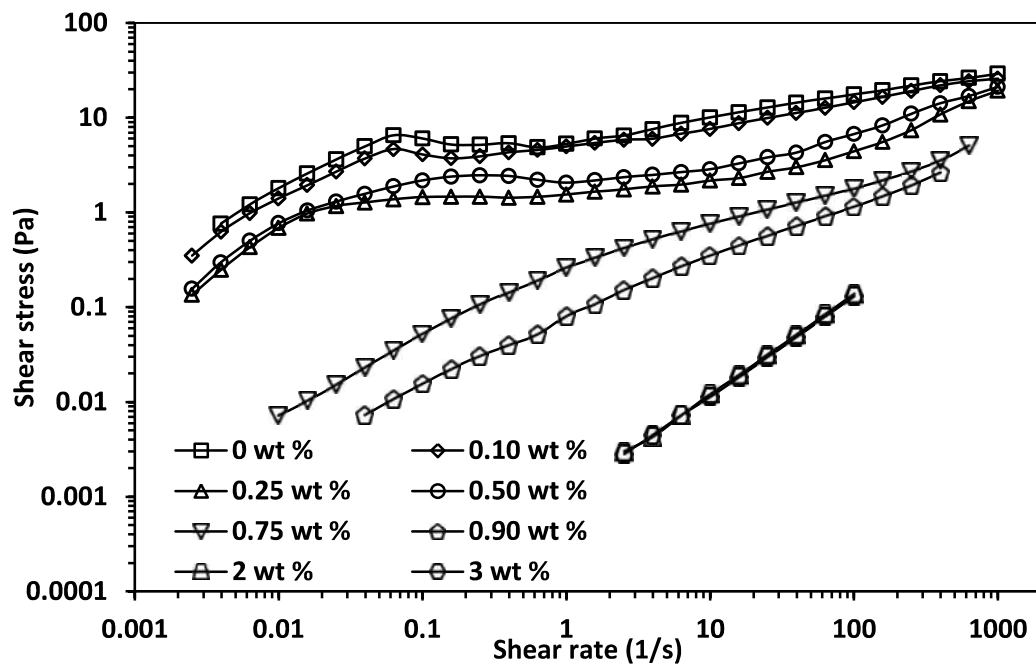


Figure 38 Shear stress vs shear rate of 3.96 wt % surfactant solution with different concentrations of n-decane at 30°C

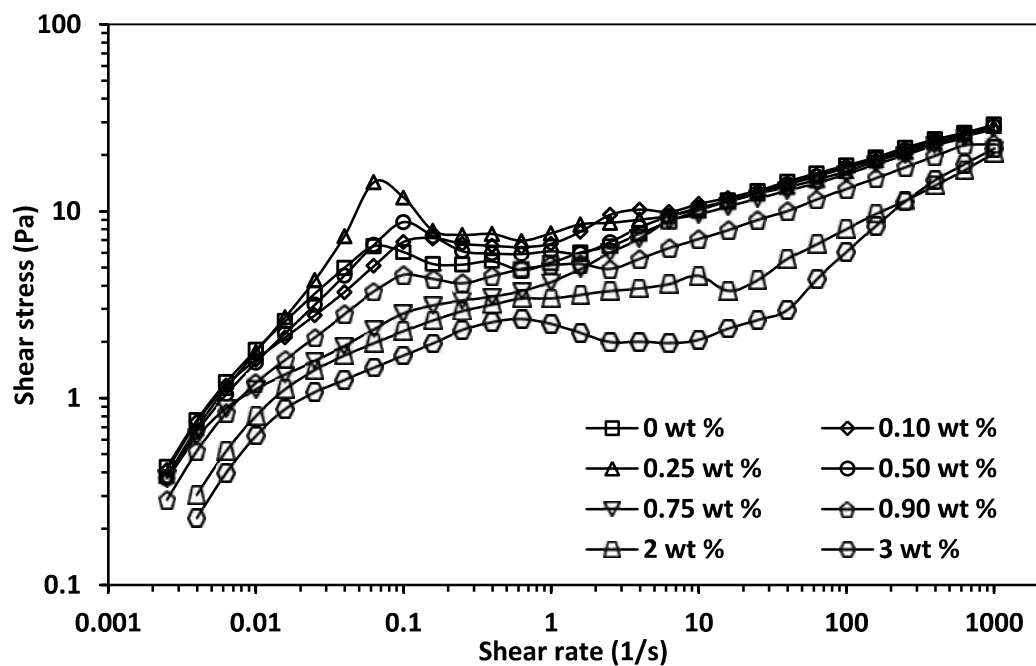


Figure 39 Shear stress vs shear rate of 3.96 wt % surfactant solution with different concentrations of crude oil at 30°C

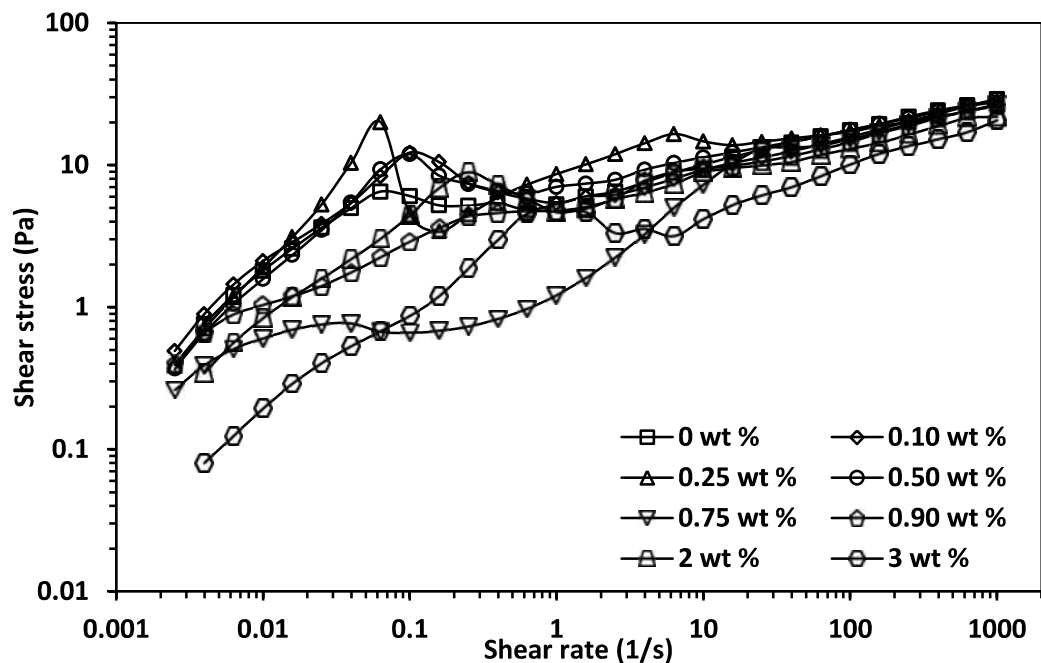


Figure 40 Shear stress vs shear rate of 3.96 wt % surfactant solution with different concentrations of EVOO at 30°C

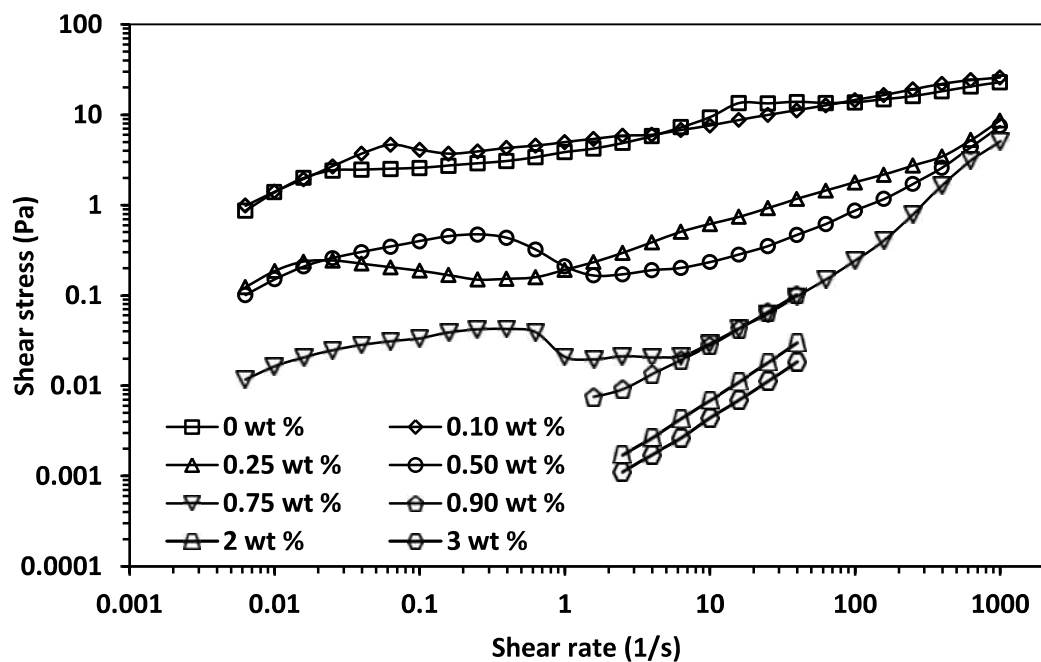


Figure 41 Shear stress vs shear rate of 3.96 wt % surfactant solution with different concentrations of n-decane at 60°C

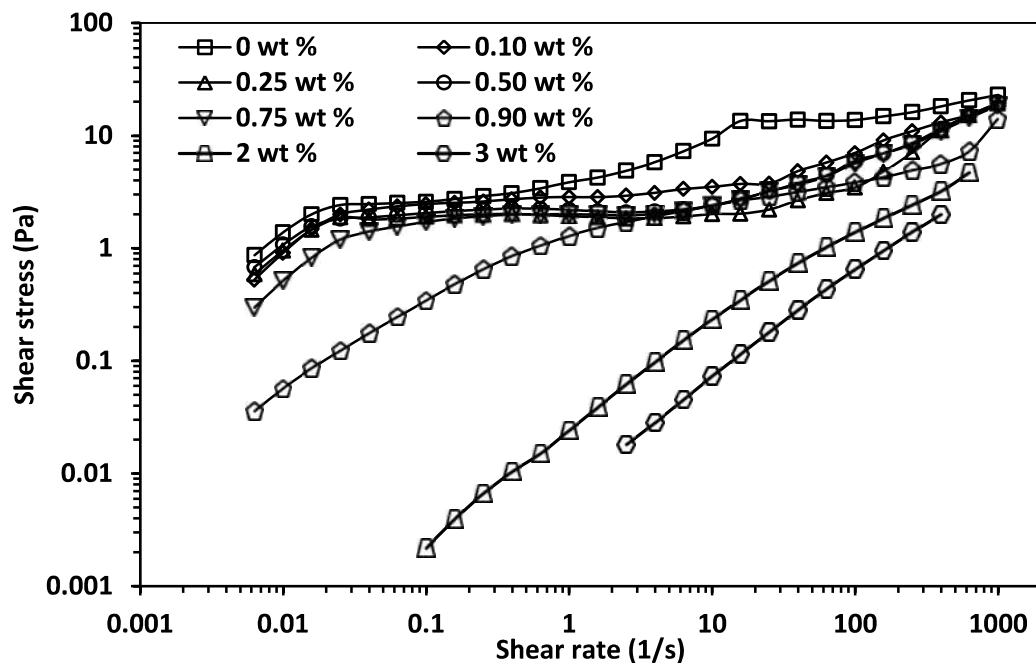


Figure 42 Shear stress vs shear rate of 3.96 wt % surfactant solution with different concentrations of crude oil at 60°C

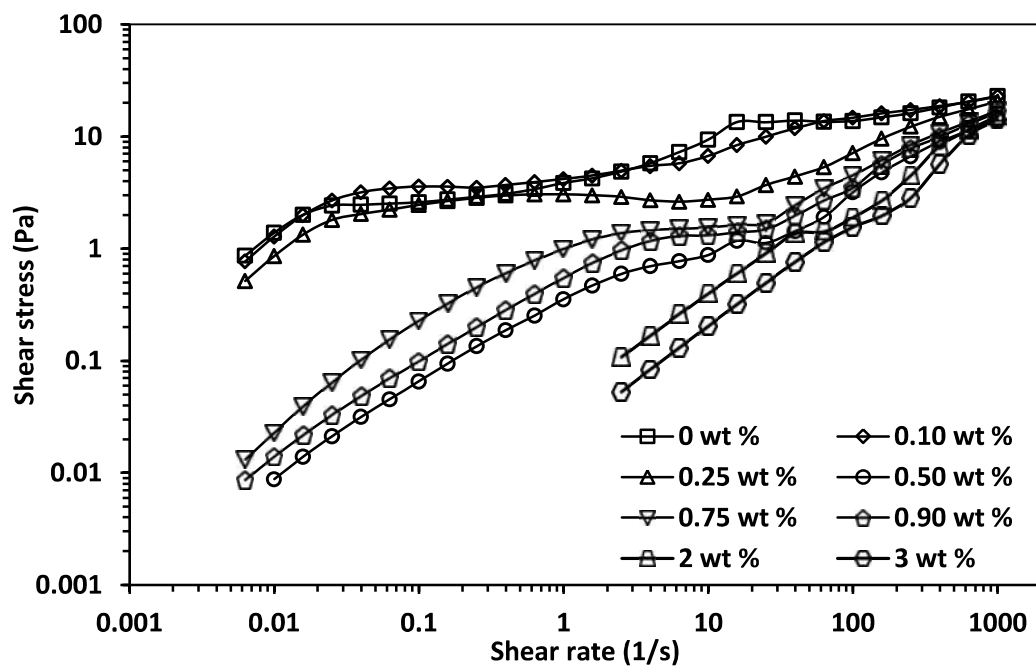


Figure 43 Shear stress vs shear rate of 3.96 wt % surfactant solution with different concentrations of EVOO at 60°C

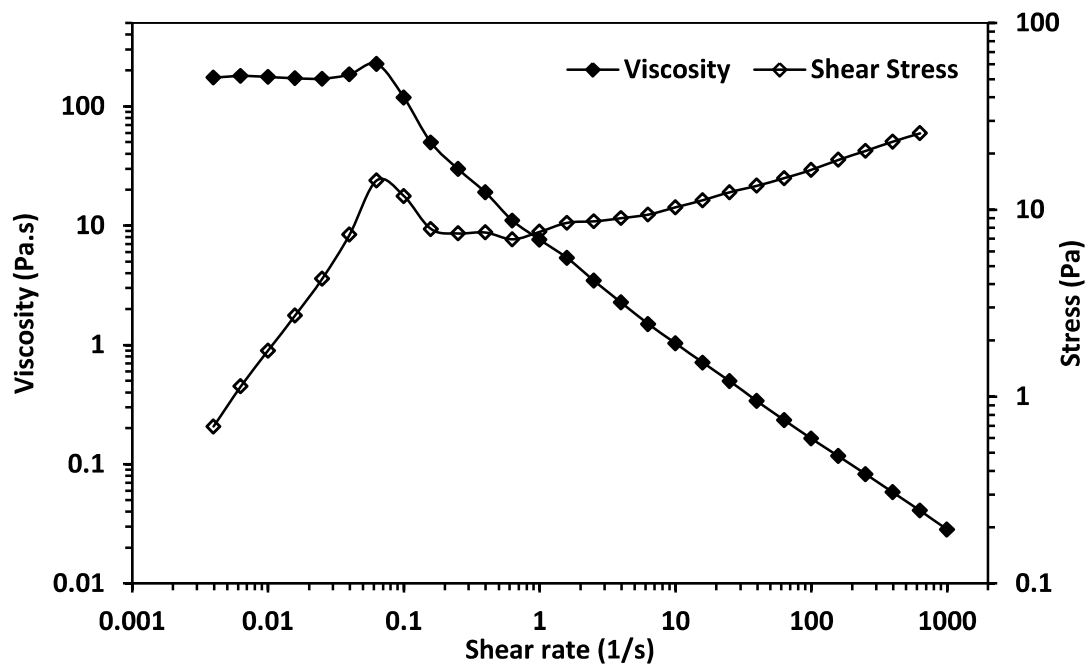


Figure 44 Viscosity and stress vs shear rate of 3.96 wt % surfactant solution with 0.25 wt% crude oil at 30°C.

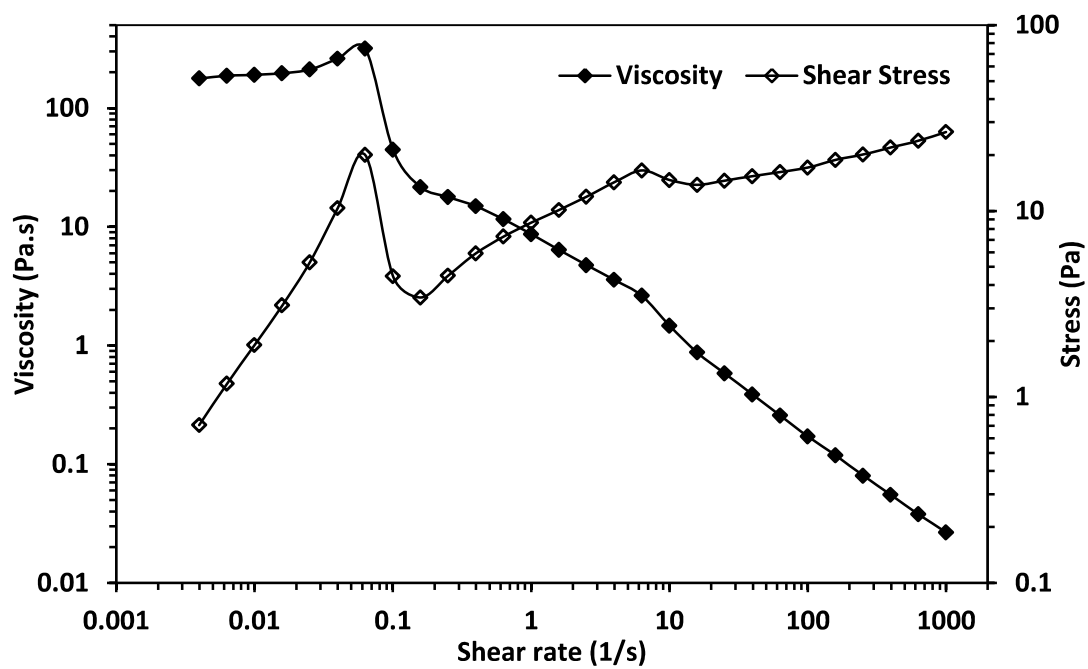


Figure 45 Viscosity and stress vs shear rate of 3.96 wt % surfactant solution with 0.25 wt% EVOO at 30°C

At 60°C, the HVR existed mainly due to the low concentrations of the oils as more oil molecules had enough kinetic energy to penetrate the micelles. This is inferred from the fact that concentration range of the oils for the HVR at 60°C was 0.1-0.5 wt %.

The transition regime: The following oil concentration ranges delineated the TR: (i) 0.5-2 wt % n-decane at 30°C (Figure 22), (ii) 0.5-0.9 wt % n-decane at 60°C (Figure 22), (iii) 0.5-3 wt % of crude oil and EVOO at 60°C (Figure 23-Figure 24). There was a sharp drop in zero-shear viscosity with increasing oil concentration in this regime. Untangled cylindrical micelles in the surfactant solutions with these oil concentrations characterize this regime. The presence of cylindrical micelles is inferred from the transitions from the Newtonian to the shear-thinning region with increasing shear rate at these oil concentrations (Figure 26, Figure 29-Figure 31). Evidence for untangled cylindrical micelles is from the absence of G_0 and G''_{min} from the dynamic shear rheology plots at these oil concentrations (Figure 32, Figure 35-Figure 37). These absences imply deviations from the Maxwellian fluid model [18].

The presence of untangled micelles signify that the cylindrical micelles have been shortened; short micelles cannot entangle with each other [18]. Cryo-TEM revealed the presence of short cylindrical micelles in the surfactant solutions with 0.9 wt% n-decane equilibrated at 30°C (Figure 46). The existence of the TR at both temperatures was mainly because the oil concentrations were enough to prevent the formation of dense micelle networks during the equilibration period by shortening the long micelles.

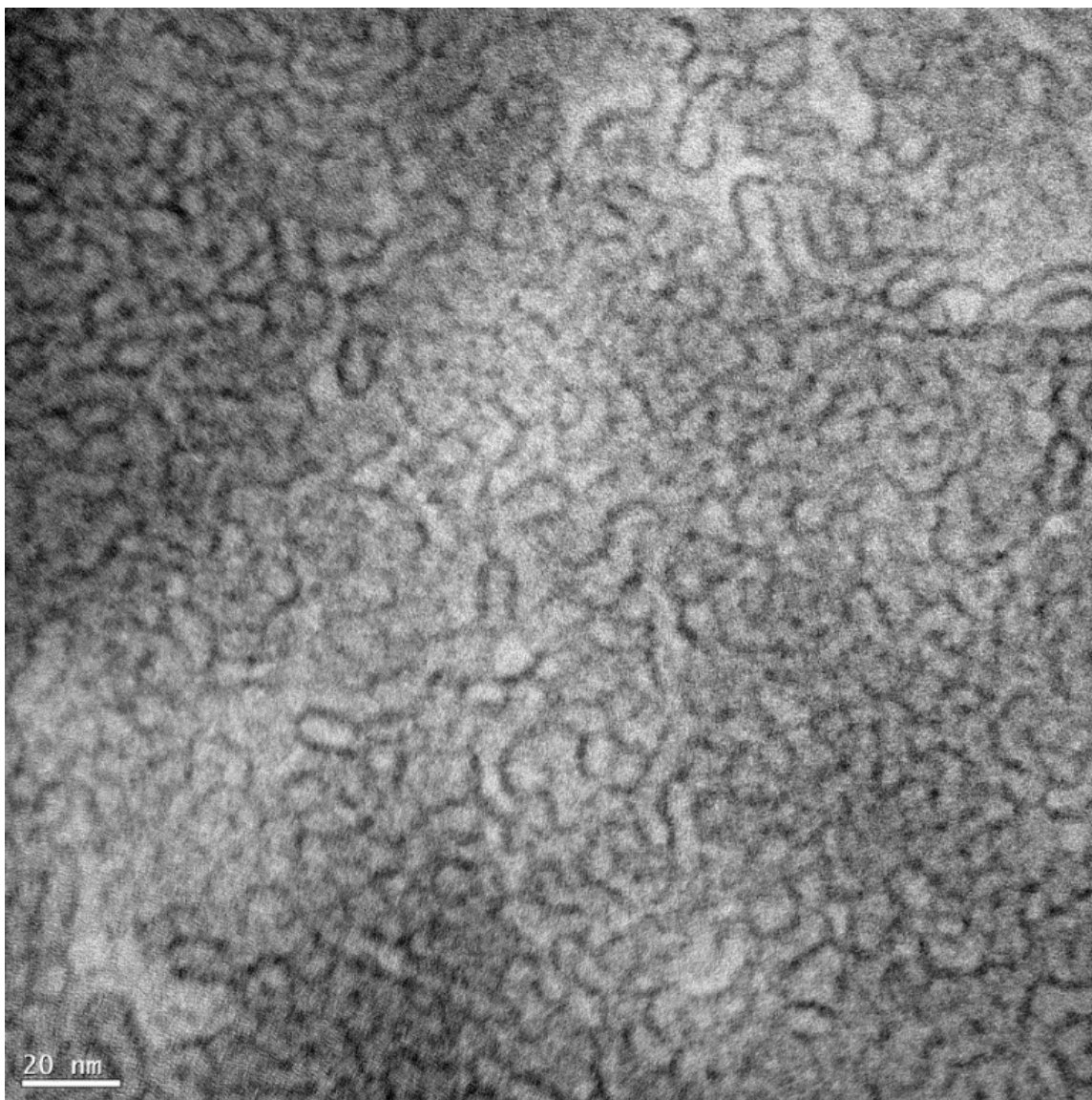


Figure 46 Cryo-TEM image of 3.96 wt % surfactant solution with 0.9 wt % n-decane at 30°C. The black curves are the edges of the micelles.

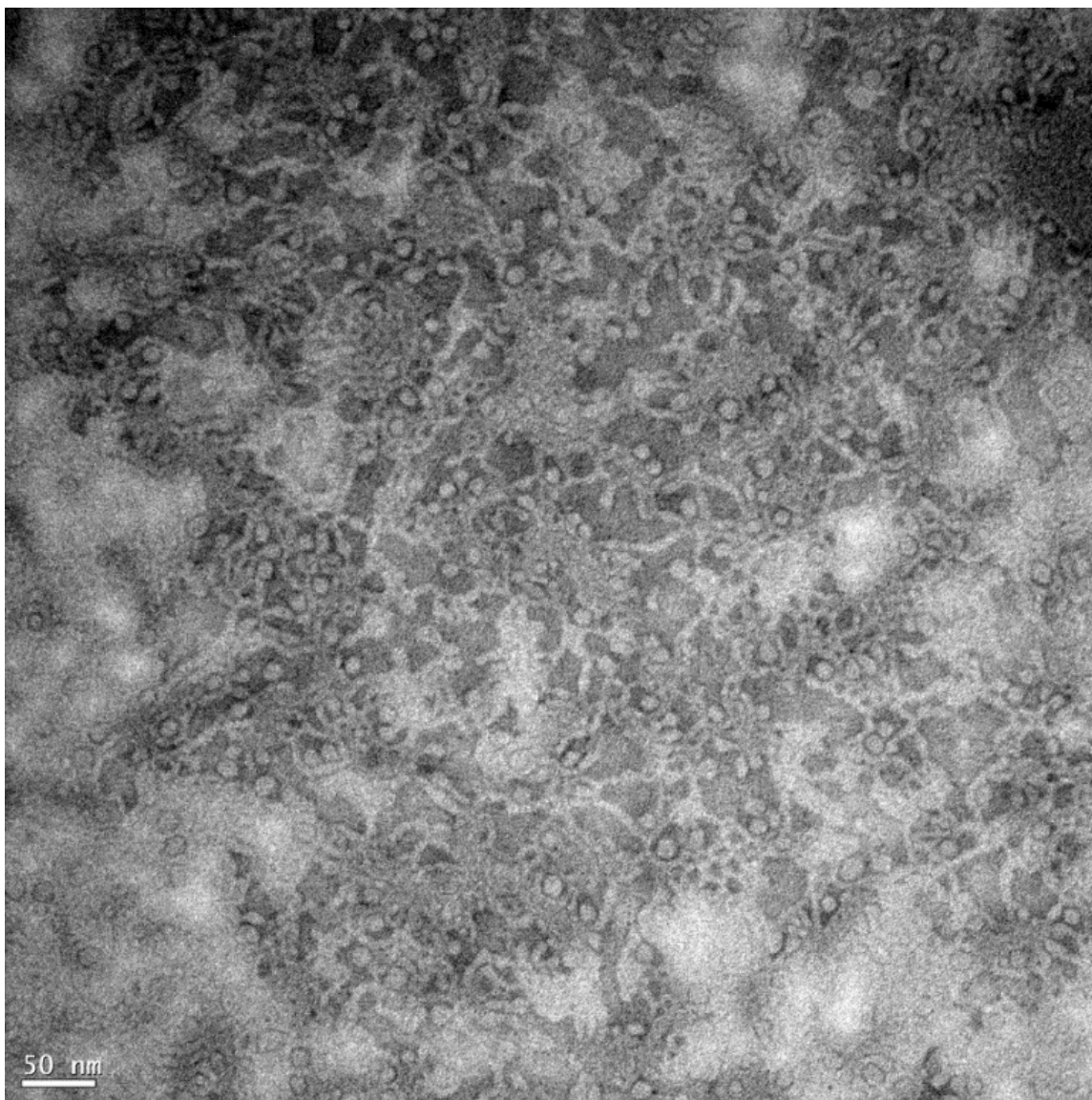


Figure 47 Cryo-TEM image of 3.96 wt % surfactant solution with 3 wt % n-decane at 60°C. The white sections represent the micelles

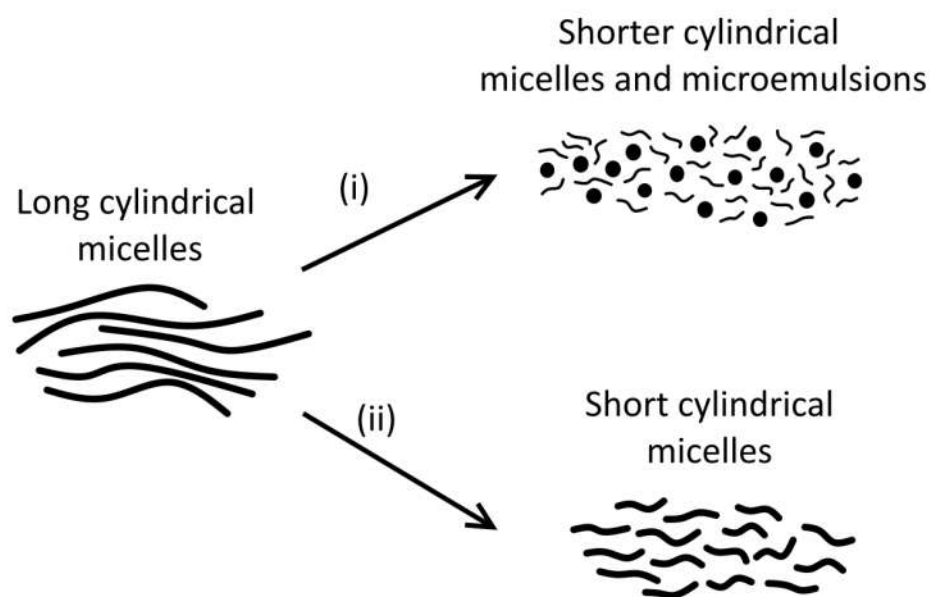


Figure 48 Schematic of the effect of (i) 3 wt % n-decane and (ii) 3 wt % crude oil and EVOO on the cylindrical micelles at 60°C

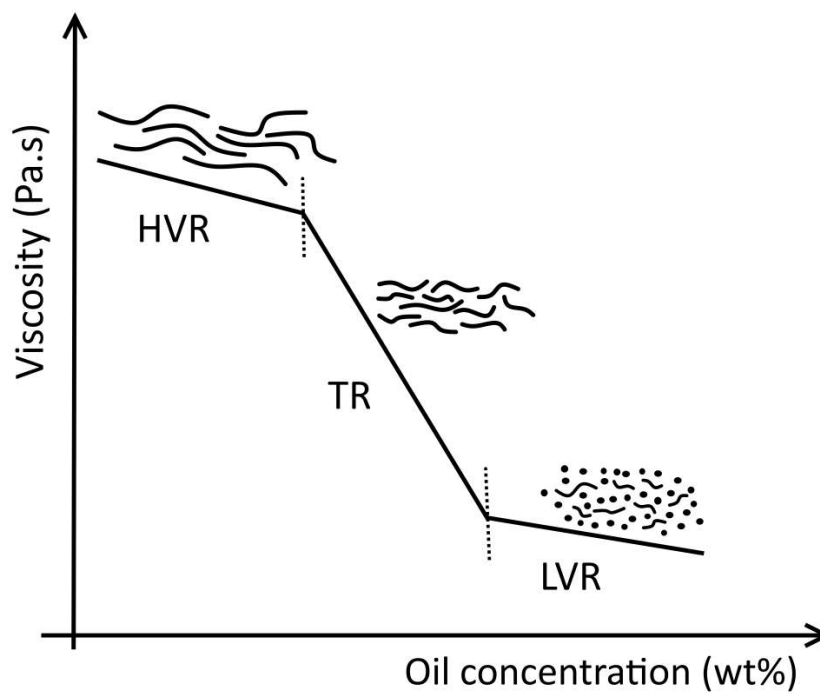


Figure 49 Schematic representation of micelle transitions induced by the oils at 30°C and 60°C

The low viscosity regime: The following n-decane concentration ranges delineated the LVR: (i) 2-3 wt % at 30°C (Figure 22), (ii) 0.9-3 wt % at 60°C (Figure 22). Surfactant solutions with these n-decane concentrations exhibited Newtonian fluid behavior; the viscosity remained constant with increasing shear rate (Figure 26, Figure 29). This is evidence that microemulsions were present in these solutions [18], [38]–[40]. Cryo-TEM revealed the presence of microemulsions in the surfactant solution with 3 wt % n-decane equilibrated at 60°C (Figure 47). The LVR existed at both temperatures because there were sufficient n-decane molecules for the cylindrical micelles to capture and turn into microemulsions.

Schematic representations of the micelle shape transitions induced by the oils are shown in Figure 48 and Figure 49.

5.2.2 Effect of PGA

The viscosity with shear rate plot of the surfactant solution with 0.1-0.9 wt % of PGA at 30°C and 60°C is shown in Figure 50 and Figure 51, respectively. There were no drastic changes in zero-shear viscosity with increasing PGA concentrations when compared to increasing concentrations of n-decane at 30°C. Moreover, the changes in zero-shear viscosity at 60°C were insignificant compared to the changes induced by the oils at the same temperature. These trends in zero-shear viscosity are represented more clearly in Figure 52. The transition from the Newtonian to the shear-thinning region at these concentrations was less smooth at 30°C than at 60°C. This means the cylindrical micelles were more entangled at 30°C than at 60°C.

The variation of G' and G'' with angular frequency of the surfactant solution with 0.1-0.9 wt % of PGA at 30°C and 60°C are shown in Figures Figure 53 and Figure 54, respectively. The behavior of G' and G'' was also similar to that of the pure surfactant solution at 30°C. The crossover frequency and the regions in which G'' dominates G' at lower angular frequencies were absent at 30°C. The reason for this absence is the same as that of the pure surfactant solution at 30°C. At 60°C, the crossover frequency was present at 0.9 wt % PGA, meaning that the crossover frequency of surfactant solution increased with increasing concentration of PGA. Therefore, PGA insignificantly affected the micelle structure of the surfactant solution.

The effect of PGA on this surfactant can be understood by comparing the effect of PGA on the amphoteric carboxylic betaine surfactant, EDAB [35]. Amphoteric carboxylic betaine surfactants become cationic or anionic at low and high pH, respectively [64], [65], unlike sulfobetaine surfactants that remain zwitterionic at all pH [65]. Increasing PGA concentrations reduce the pH of the EDAB solution, turning the surfactant from amphoteric to cationic. This change increases the charge of the headgroup and increases the effective headgroup area. The increase in effective headgroup area reduces the packing parameter (based on equation 1), causing the EDAB micelle to change from a cylindrical to spherical. The effect of changing the headgroup charge was also proposed for the changes in micelle structure induced by NaSal and NaHNC on EDAB [39]. Because sulfobetaine surfactant solutions remain zwitterionic with a decrease in pH, their micellar structure will not undergo significant changes [58].

Thus, the decrease in pH by PGA did not significantly affect the micelle structure of the surfactant solution. This reflected in the insignificant changes in zero-shear viscosity

induced by PGA when compared to the oils. A schematic representation of this insignificant change is shown in Figure 55.

5.3 Implications for well stimulation

The oils tested are breakers for this surfactant system at high temperatures. Temperature significantly improves the ability of the heavy molecular weight oils to break the surfactant solution and reduces the amount of breakers needed for breaking. Thus, the breaker concentration needed for VES-based well stimulation will depend on the reservoir temperature.

Considering the responsiveness of the surfactant solution to crude oil implies that the amount of internal breaker needed for well cleanup in crude oil formations will reduce.

When a VES is used for well stimulation, the optimum breaking time should be at the end of the well stimulation job. The breaker concentration needed for viscosity reduction of the VES gel can be controlled to fit the optimum breaking time. The optimum breaker concentration should also account for the breaking effect of reservoir crude oil if the well is located in crude oil reservoirs.

The responsiveness of the surfactant solution to n-decane and EVOO shows that the surfactant is responsive to crude oils that contain C10-C18 molecules. Moreover, the responsiveness of the surfactant gel to EVOO also shows that well stimulation using these fluids will not be environmentally detrimental; both the surfactant system and EVOO are environmentally friendly.

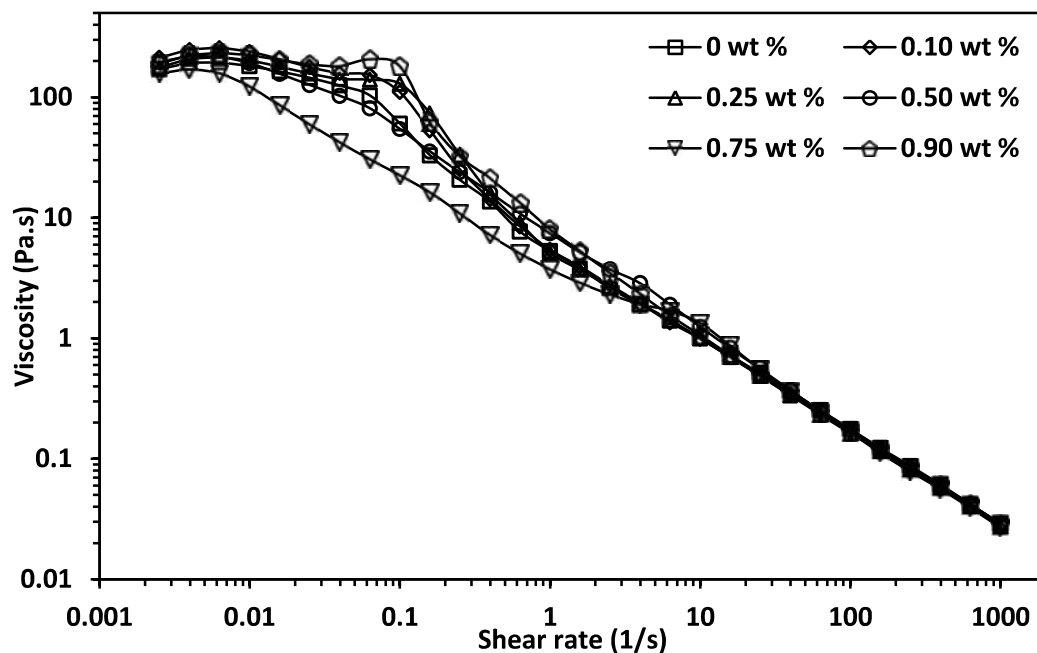


Figure 50 Viscosity vs shear rate of 3.96 wt % surfactant solution with different concentrations of PGA at 30°C

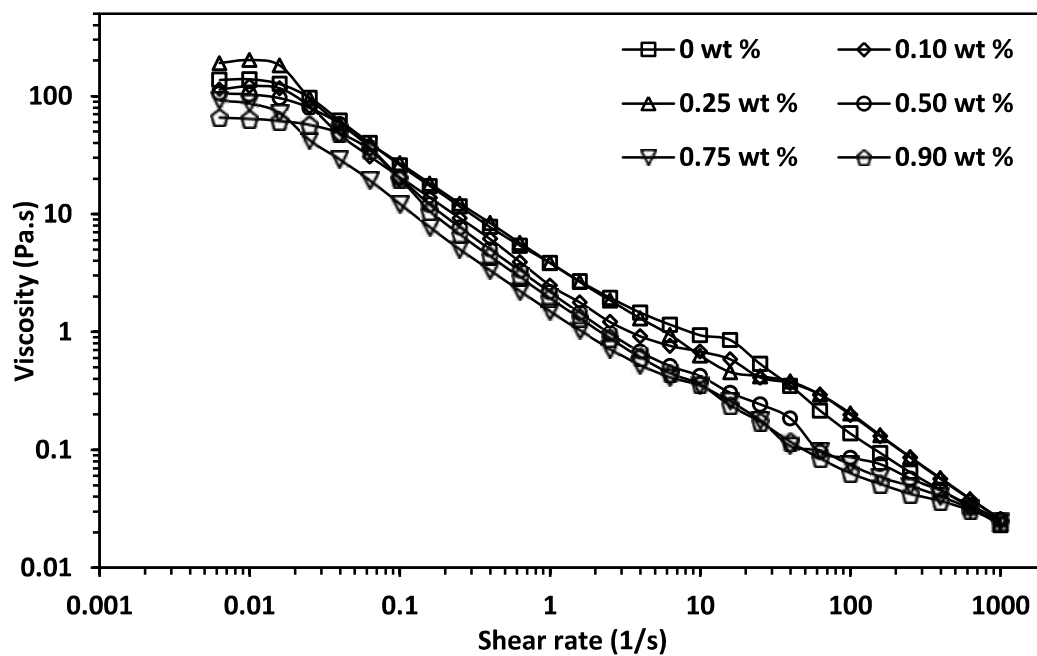


Figure 51 Viscosity vs shear rate of 3.96 wt % surfactant solution with different concentrations of PGA at 60°C

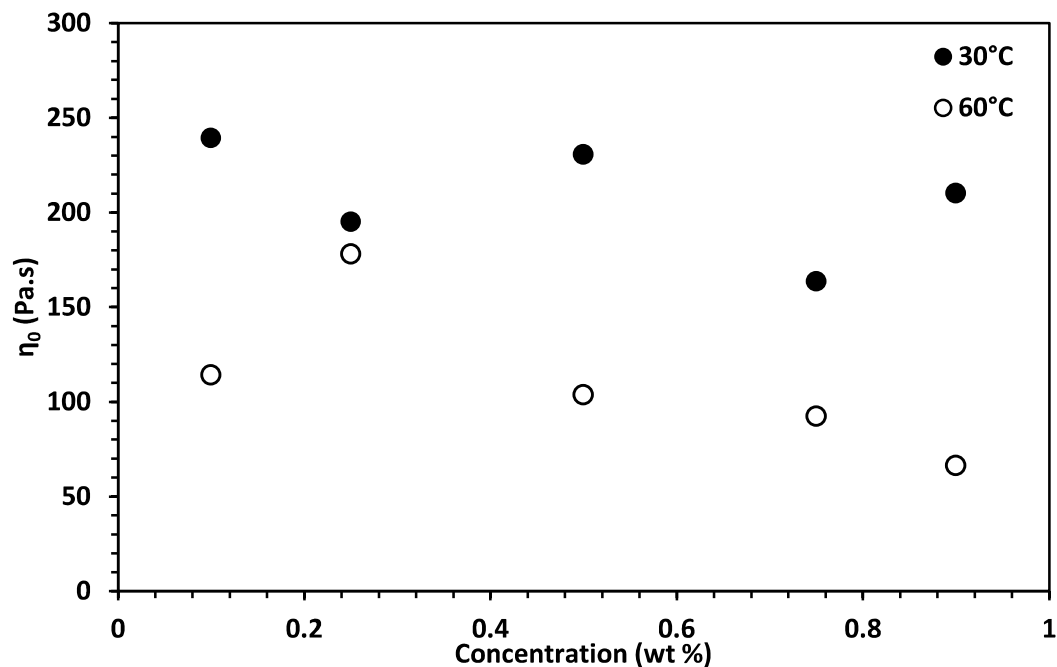


Figure 52 Estimated zero-shear viscosity of 3.96 wt % surfactant solution with different PGA concentrations

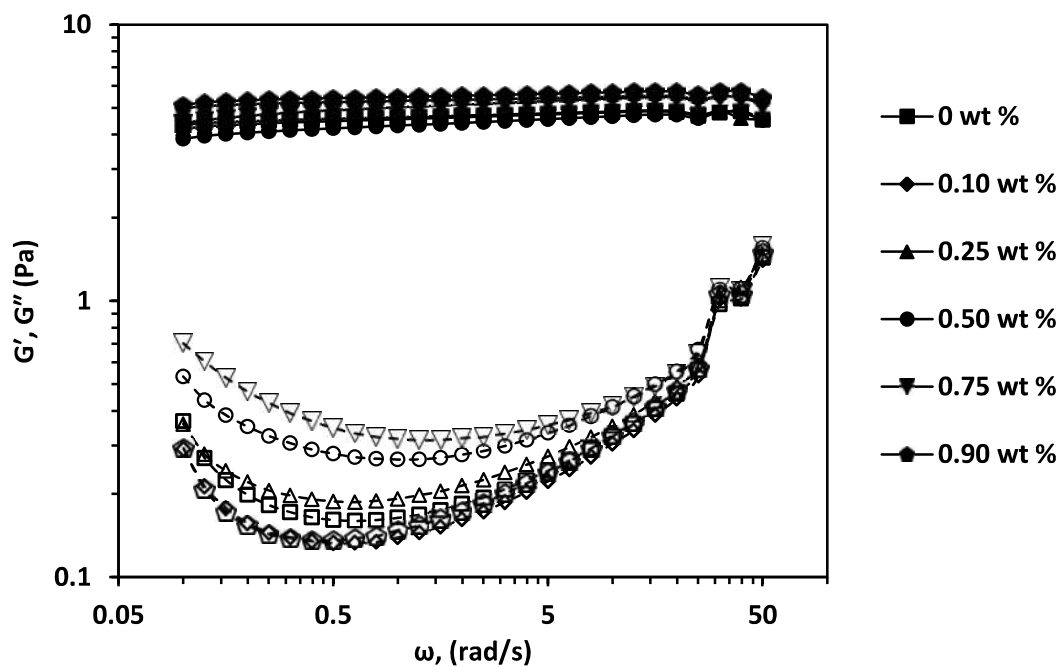


Figure 53 Storage modulus (filled symbols) and loss modulus (open symbols) of 3.96 wt % surfactant with different concentrations of PGA at 30°C

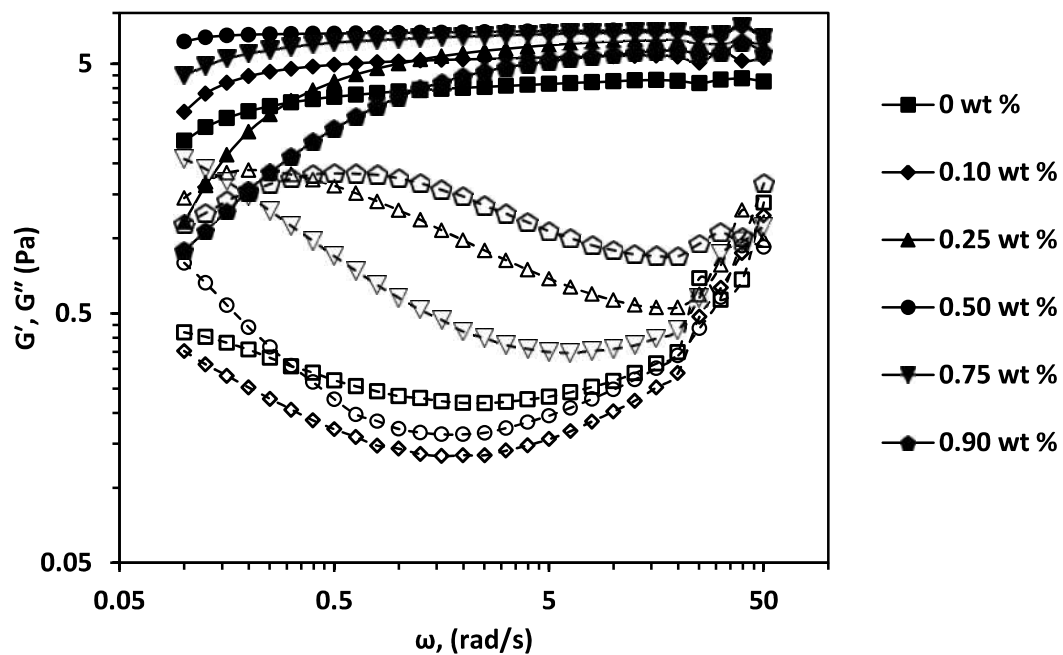


Figure 54 Storage modulus (filled symbols) and loss modulus (open symbols) of 3.96 wt % surfactant with different concentrations of PGA at 60°C

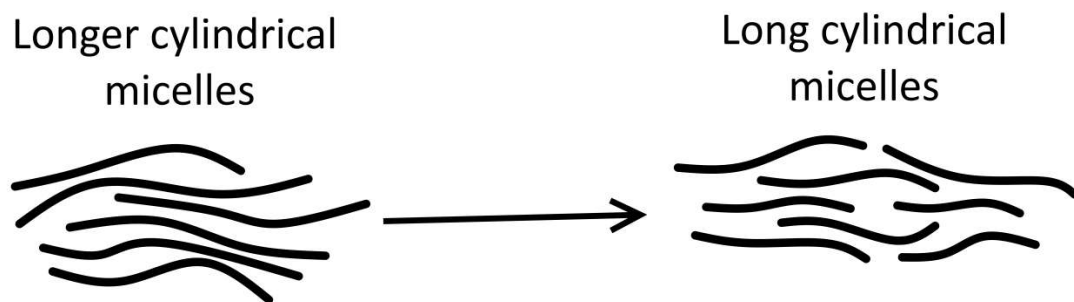


Figure 55 Schematic representing the effect of 0.9 wt % PGA on the cylindrical micelles at 60°C

CHAPTER 6

CONCLUSIONS

The surfactant solution with 3.96 wt % of the sulfobetaine surfactant system and 6.2 wt % CaCl_2 has a viscoelastic behavior at 30°C and 60°C after one week of equilibration. This is due to the formation of cylindrical micelles. The cylindrical micelles are more entangled at 30°C than at 60°C, making the surfactant solution more viscous at 30°C.

Breaker concentration and temperature increases the breaking capacity of the oils. Only n-decane drastically affects the zero-shear viscosity of the surfactant solution at 30°C. The oils drastically affect the zero-shear viscosity of the surfactant solutions at 60°C. At 60°C, the zero-shear viscosity of the surfactant solution decreases with increasing concentrations of the oils at 60°C, with the effect of n-decane surpassing that of crude oil and EVOO. The reduction in viscosity with increasing oil concentrations can be separated into different regimes that represent a change in micelle structure. The regimes are the high viscosity regime, the transition regime, and the low viscosity regime. The existence of each regime depends on the balance between micellization and oil solubilization. PGA does not induce significant changes in viscosity on this VES system, and it is primarily due to the resistance of the VES to changing pH.

The recommendations for well stimulation operations are as follows:

1. Crude oil should not be relied on as the only breaking fluid in well stimulation.

2. Breaker concentrations should be chosen based on the reservoir temperature and the time required for the stimulation job to be completed. These breaker concentrations should take into account the breaking ability of the formation oil.
3. The choice of oil to be used as a breaker should depend on its molecular structure, cost, and its environmental impact.
4. PGA should not be used as breakers for this sulfobetaine surfactant system.

References

- [1] M. J. Rosen and J. T. Kunjappu, "Characteristic Features of Surfactants," in *Surfactants and Interfacial Phenomena*, John Wiley & Sons, Inc., 2012, pp. 1–38.
- [2] L. L. Schramm, E. N. Stasiuk, and D. G. Marangoni, "2 Surfactants and their Applications," *Annu. Rep. Sect. C Phys. Chem.*, vol. 99, p. 3, 2003.
- [3] O. Soderman, P. Stilbs, and W. S. Price, "NMR Studies of Surfactants," *Concepts Magn. Reson.*, vol. 23A, no. 2, pp. 121–135, Nov. 2004.
- [4] F. M. Menger and C. A. Littau, "Gemini surfactants: a new class of self-assembling molecules," *J. Am. Chem. Soc.*, vol. 115, no. 22, pp. 10083–10090, Nov. 1993.
- [5] H. Rehage and H. Hoffmann, "Rheological Properties of Viscoelastic Surfactant Systems," *J. Phys. Chem.*, vol. 92, no. 16, pp. 4712–4719, 1988.
- [6] R. Ravitz, L. Moore, and C. Svoboda, "VES: An Alternative to Biopolymers in Reservoir Drill-In Fluids," presented at the 8th European Formation Damage Conference, Scheveningen, The Netherlands, 2009.
- [7] S. Kefi, J. Lee, T. Pope, P. Sullivan, E. Nelson, A. Hernandez, T. Olsen, M. Parlar, B. Powers, and A. Roy, "Expanding Applications for Viscoelastic Surfactants," *Oilfield Rev.*, vol. 16, no. 4, pp. 10–23, 2004.
- [8] J. Crews and T. Huang, "Internal Breakers for Viscoelastic-Surfactant Fracturing Fluids," presented at the International Symposium on Oilfield Chemistry, Houston, Texas, 2007.
- [9] M. Samuel, R. Card, E. Nelson, J. Brown, P. S. Vinod, H. Temple, Q. Qu, and D. Fu, "Polymer-Free Fluid for Hydraulic Fracturing," presented at the SPE Annual Technical Conference and Exhibition, San Antonio, Texas, 1997.
- [10] D. Gupta, "Unconventional Fracturing Fluids for Tight Gas Reservoirs," presented at the SPE Hydraulic Fracturing Technology Conference, The Woodlands, Texas, 2009.
- [11] H. Nasr-El-Din, S. Al-Driweesh, K. Bartko, H. Al-Ghadhban, V. Ramanathan, S. Kelkar, and M. Samuel, "Acid Fracturing of Deep Gas Wells Using a Surfactant-Based Acid: Long-Term Effects on Gas Production Rate," presented at the SPE Annual Technical Conference and Exhibition, San Antonio, Texas, 2006.
- [12] M. Samuel, D. Polson, D. Graham, W. Kordziel, T. Waite, G. Waters, P. S. Vinod, D. Fu, and R. Downey, "Viscoelastic Surfactant Fracturing Fluids: Applications in Low Permeability Reservoirs," presented at the SPE Rocky Mountain Regional/Low-Permeability Reservoirs Symposium and Exhibition, Denver, Colorado, 2000.
- [13] F. Chang, Q. Qu, and W. Frenier, "A Novel Self-Diverting-Acid Developed for Matrix Stimulation of Carbonate Reservoirs," presented at the SPE International Symposium on Oilfield Chemistry, Houston, Texas, 2001.
- [14] M. Al-Mutawa, E. Al-Anzi, M. Jemmali, F. Chang, E. Samuel, and M. Samuel, "Zero-Damaging Stimulation and Diversion Fluid: Field Cases From the Carbonate Formations in North Kuwait," *SPE Prod. Facil.*, vol. 20, no. 2, May 2005.

- [15] C. Zeiler, D. Alleman, and Q. Qu, "Use of Viscoelastic-Surfactant-Based Diverting Agents for Acid Stimulation: Case Histories in GOM," *SPE Prod. Oper.*, vol. 21, no. 4, Nov. 2006.
- [16] A. Al-Ghamdi, M. Mahmoud, A. Hill, and H. Nasr-El-Din, "When Do Surfactant-Based Acids Work as Diverting Agents?," presented at the SPE International Symposium and Exhibiton on Formation Damage Control, Lafayette, Louisiana, 2010.
- [17] T. Huang and D. Clark, "Advanced Fluid Technologies for Tight Gas Reservoir Stimulation," presented at the SPE Saudi Arabia Section Technical Symposium and Exhibition, Al-Khobar, Saudi Arabia, 2012.
- [18] A. V. Shibaev, M. V. Tamm, V. S. Molchanov, A. V. Rogachev, A. I. Kuklin, E. E. Dormidontova, and O. E. Philippova, "How a Viscoelastic Solution of Wormlike Micelles Transforms into a Microemulsion upon Absorption of Hydrocarbon: New Insight," *Langmuir*, vol. 30, no. 13, pp. 3705–3714, Apr. 2014.
- [19] D. Danino, A. Bernheim-Groswasser, and Y. Talmon, "Digital Cryogenic Transmission Electron Microscopy: An Advanced Tool for Direct Imaging of Complex Fluids," *Colloids Surf. Physicochem. Eng. Asp.*, vol. 183, pp. 113–122, 2001.
- [20] C. O. Rangel-Yagui, A. Pessoa Jr, and L. C. Tavares, "Micellar Solubilization of Drugs," *J Pharm Pharm Sci*, vol. 8, no. 2, pp. 147–163, 2005.
- [21] P. S. Goyal and V. K. Aswal, "Micellar Structure and Inter-micelle Interactions in Micellar Solutions: Results of Small Angle Neutron Scattering Studies," *Curr. Sci.-BANGALORE*, vol. 80, no. 8, pp. 972–979, 2001.
- [22] F. F. Chang, R. L. Thomas, and D. K. Fu, "A New Material and Novel Technique for Matrix Stimulation in High-Water-Cut Oil Wells," presented at the SPE Formation Damage Control Conference, Lafayette, Louisiana, 1998.
- [23] F. F. Chang, Q. Qu, and M. J. Miller, "Fluid System Having Controllable Reversible Viscosity," 6,399,546, Jun-2002.
- [24] Y. Feng, Z. Chu, and C. A. Dreiss, "Basic Properties of Wormlike Micelles," in *Smart Wormlike Micelles*, Springer Berlin Heidelberg, 2015, pp. 1–6.
- [25] T. Huang and J. Crews, "Do Viscoelastic-Surfactant Diverting Fluids for Acid Treatments Need Internal Breakers?," in *SPE International Symposium and Exhibition on Formation Damage Control*, Lafayette, Louisiana, 2008.
- [26] M. Yu, M. Mahmoud, and H. Nasr-El-Din, "Propagation and Retention of Viscoelastic Surfactants Following Matrix Acidizing Treatments in Carbonate Cores," presented at the SPE International Symposium and Exhibiton on Formation Damage Control, Lafayette, Louisiana, 2010.
- [27] C. Abad, J. C. Lee, P. F. Sullivan, E. Nelson, Y. Chen, B. Baser, and L. Lin, "Internal Breaker for Oilfield Treatments," US7857051 B2, 28-Dec-2010.
- [28] J. B. Crews, "Metal-Mediated Viscosity Reduction of Fluids Gelled with Viscoelastic Surfactants," 23-Feb-2006.
- [29] J. B. Crews, "Saponified Fatty Acids as Breakers for Viscoelastic Surfactant-gelled Fluids," US8236864 B2, 07-Aug-2012.
- [30] J. B. Crews and T. Huang, "Unsaturated Fatty Acids and Mineral Oils as Internal Breakers for VES-gelled Fluids," US8101557 B2, 24-Jan-2012.

- [31] L. Li, L. Lin, C. Abad, and T. Bui, "Acidic Internal Breaker for Viscoelastic Surfactant Fluids in Brine," US7635028 B2, 22-Dec-2009.
- [32] L. Lin, Y. Chen, P. F. Sullivan, B. Baser, C. Abad, and J. C. Lee, "Oxidative Internal Breaker for Viscoelastic Surfactant Fluids," US7879770 B2, 01-Feb-2011.
- [33] L. Lin, L. Li, and C. Abad, "Internal Breakers for Viscoelastic Surfactant Fluids," US8067342 B2, 29-Nov-2011.
- [34] P. F. Sullivan, B. Baser, C. Abad, Y. Chen, M. Parlar, and G. Kubala, "Internal Breaker for Oilfield Fluids," US7431087 B2, 07-Oct-2008.
- [35] P. F. Sullivan, J. E. Brown, J. C. Lee, and G. Salamat, "Degradable Additive for Viscoelastic Surfactant Based Fluid Systems," US7219731 B2, 22-May-2007.
- [36] Z. Lin and C. D. Eads, "Polymer-induced Structural Transitions in Oleate solutions: Microscopy, Rheology, and Nuclear Magnetic Resonance Studies," *Langmuir*, vol. 13, no. 10, pp. 2647–2654, 1997.
- [37] T. Sato, D. P. Acharya, M. Kaneko, K. Aramaki, Y. Singh, M. Ishitobi, and H. Kunieda, "Oil-Induced Structural Change of Wormlike Micelles in Sugar Surfactant Systems," *J. Dispers. Sci. Technol.*, vol. 27, no. 5, pp. 611–616, Aug. 2006.
- [38] V. S. Molchanov, O. E. Philippova, A. R. Khokhlov, Y. A. Kovalev, and A. I. Kuklin, "Self-Assembled Networks Highly Responsive to Hydrocarbons," *Langmuir*, vol. 23, no. 1, pp. 105–111, Jan. 2007.
- [39] R. Kumar, G. C. Kalur, L. Ziserman, D. Danino, and S. R. Raghavan, "Wormlike Micelles of a C22-Tailed Zwitterionic Betaine Surfactant: From Viscoelastic Solutions to Elastic Gels," *Langmuir*, vol. 23, no. 26, pp. 12849–12856, Dec. 2007.
- [40] S. C. Sharma, R. G. Shrestha, L. K. Shrestha, and K. Aramaki, "Viscoelastic Wormlike Micelles in Mixed Nonionic Fluorocarbon Surfactants and Structural Transition Induced by Oils," *J. Phys. Chem. B*, vol. 113, no. 6, pp. 1615–1622, Feb. 2009.
- [41] P. A. Kralchevsky, N. D. Denkov, P. D. Todorov, G. S. Marinov, G. Broze, and A. Mehreteab, "Kinetics of Triglyceride Solubilization by Micellar Solutions of Nonionic Surfactant and Triblock Copolymer. 2. Theoretical Model," *Langmuir*, vol. 18, no. 21, pp. 7887–7895, Oct. 2002.
- [42] P. D. Todorov, P. A. Kralchevsky, N. D. Denkov, G. Broze, and A. Mehreteab, "Kinetics of Solubilization of n-Decane and Benzene by Micellar Solutions of Sodium Dodecyl Sulfate," *J. Colloid Interface Sci.*, vol. 245, no. 2, pp. 371–382, Jan. 2002.
- [43] P. D. Todorov, G. S. Marinov, P. A. Kralchevsky, N. D. Denkov, P. Durbut, G. Broze, and A. Mehreteab, "Kinetics of Triglyceride Solubilization by Micellar Solutions of Nonionic Surfactant and Triblock Copolymer. 3. Experiments with Single Drops," *Langmuir*, vol. 18, no. 21, pp. 7896–7905, Oct. 2002.
- [44] W. Siriawatwechakul, T. LaFleur, R. K. Prud'homme, and P. Sullivan, "Effects of Organic Solvents on the Scission Energy of Rodlike Micelles," *Langmuir*, vol. 20, no. 21, pp. 8970–8974, Oct. 2004.
- [45] A. I. Malkin and A. I. Isayev, *Rheology: Concepts, Methods, and Applications*. Toronto, Ont.: ChemTec Pub., 2006.
- [46] D. Weitz, H. Wyss, and R. Larsen, "Oscillatory Rheology: Measuring the Viscoelastic Behaviour of Soft Materials," *GIT Lab. J. Eur.*, vol. 11, no. 3–4, pp. 68–70, 2007.

- [47] R. Zana, Ed., *Dynamics of Surfactant Self-Assemblies: Micelles, Microemulsions, Vesicles and Lyotropic Phases*. CRC Press, 2005.
- [48] M. E. Cates and S. J. Candau, "Statics and dynamics of worm-like surfactant micelles," *J. Phys. Condens. Matter*, vol. 2, no. 33, p. 6869, 1990.
- [49] R. Granek and M. E. Cates, "Stress relaxation in living polymers: Results from a Poisson renewal model," *J. Chem. Phys.*, vol. 96, no. 6, pp. 4758–4767, Mar. 1992.
- [50] M. Almgren, K. Edwards, and J. Gustafsson, "Cryotransmission Electron Microscopy of Thin Vitrified Samples," *Curr. Opin. Colloid Interface Sci.*, vol. 1, no. 2, pp. 270–278, 1996.
- [51] Y. I. González and E. W. Kaler, "Cryo-TEM Studies of Worm-like Micellar Solutions," *Curr. Opin. Colloid Interface Sci.*, vol. 10, no. 5–6, pp. 256–260, Dec. 2005.
- [52] M. J. Engel, J. F. Gadberry, J. D. Nowak, X. Wang, and J. Zhou, "Thickened viscoelastic fluids and uses thereof," WO2012160008 A1, 29-Nov-2012.
- [53] M. C. Ramírez-Tortosa, S. Granados, and J. L. Quiles, "Chemical composition, types and characteristics of olive oil.," in *Olive oil and health*, J. L. Quiles, M. C. Ramírez-Tortosa, and P. Yaquob, Eds. Wallingford: CABI, 2006, pp. 45–62.
- [54] R. J. L. Sr, *Hawley's Condensed Chemical Dictionary*, 15 edition. Wiley-Interscience, 2007.
- [55] M. Mahmoud, H. Nasr-El-Din, C. De Wolf, and J. LePage, "An Effective Stimulation Fluid for Deep Carbonate Reservoirs: A Core Flood Study," presented at the International Oil and Gas Conference and Exhibition in China, Beijing, China, 2010.
- [56] M. Sayed and H. Nasr-El-Din, "Acid Treatments in High Temperature Dolomitic Carbonate Reservoirs Using Emulsified Acids: A Coreflood Study," presented at the 2013 SPE Production and Operations Symposium, Oklahoma City, Oklahoma, 2013.
- [57] M. Sayed, A. Zakaria, H. Nasr-El-Din, S. Holt, and H. Al-Malki, "Core Flood Study of a New Emulsified Acid with Reservoir Cores," presented at the SPE International Production and Operations Conference & Exhibition, Doha, Qatar, 2012.
- [58] Z. Chu, Y. Feng, X. Su, and Y. Han, "Wormlike Micelles and Solution Properties of a C22-Tailed Amidosulfobetaine Surfactant," *Langmuir*, vol. 26, no. 11, pp. 7783–7791, Jun. 2010.
- [59] V. Croce, T. Cosgrove, C. A. Dreiss, S. King, G. Maitland, and T. Hughes, "Giant Micellar Worms under Shear: A Rheological Study Using SANS," *Langmuir*, vol. 21, no. 15, pp. 6762–6768, Jul. 2005.
- [60] J.-F. Berret, "Rheology of Wormlike Micelles: Equilibrium Properties and Shear Banding Transitions," in *Molecular Gels*, R. G. Weiss and P. Terech, Eds. Springer Netherlands, 2006, pp. 667–720.
- [61] Z. Chu and Y. Feng, "Amidosulfobetaine surfactant gels with shear banding transitions," *Soft Matter*, vol. 6, no. 24, p. 6065, 2010.
- [62] Y. Zhang, P. An, and X. Liu, "A 'worm'-containing viscoelastic fluid based on single amine oxide surfactant with an unsaturated C₂₂-tail," *RSC Adv*, vol. 5, no. 25, pp. 19135–19144, 2015.

- [63] H. Hoffmann and W. Ulbricht, "Transition of Rodlike to Globular Micelles by the Solubilization of Additives," *J. Colloid Interface Sci.*, vol. 129, no. 2, pp. 388–405, 1989.
- [64] K. Kato, H. Kondo, A. Morita, K. Esumi, and K. Meguro, "Synthesis of polystyrene latex with amphoteric surfactant and its characterization," *Colloid Polym. Sci.*, vol. 264, no. 9, pp. 737–742, Sep. 1986.
- [65] T. Yoshimura, T. Ichinokawa, M. Kaji, and K. Esumi, "Synthesis and surface-active properties of sulfobetaine-type zwitterionic gemini surfactants," *Colloids Surf. Physicochem. Eng. Asp.*, vol. 273, no. 1–3, pp. 208–212, Feb. 2006.

Vitae

| | |
|---------------------|---|
| Name | :Lionel Talley Fogang |
| Nationality | :Cameroonian |
| Date of Birth | :5/16/1989 |
| Email | :lioneltalley89@yahoo.com |
| Address | C/O of Mrs Marie Delphine Fogang, P.O. Box 14935, United Nations Economic Commission for Africa, Sub- Regional Office for Central Africa, Yaounde, Cameroon |
| Academic Background | :Bachelors of Science in Petroleum Engineering from King Fahd University of Petroleum and Minerals |